

The Cambodian Mekong floodplain under future development plans and climate change

Alexander J. Horton ^{a *}, Nguyen V. K. Triet ^b, Long P. Hoang ^{c,d}, Sokchhay Heng ^{de}, Panha Hok ^{de}, Sarit Chung ^{de}, Jorma Koponen ^{ef}, Matti Kummu ^{a *}

^a Water and Development Research Group, Aalto University, Tietotie 1E, 02150 Espoo, Finland

^b GFZ German Research Centre for Geosciences, Section 4.4 Hydrology, Potsdam, 14473, Germany

^c Water Systems and Global Change Group, Wageningen University, P.O. Box 47, 6700 AA Wageningen, the Netherlands

^{dd} VNU School of Interdisciplinary Studies, Vietnam National University, 144 Xuan Thuy Str., Hanoi, Vietnam

^e Faculty of Hydrology and Water Resources Engineering, Institute of Technology of Cambodia, Russian Federation Boulevard, P.O. Box 86, 12156 Phnom Penh, Cambodia

^{ef} EIA Finland Ltd., Sinimäentie 10B, 02630 Espoo, Finland

* Corresponding authors: Alexander.horton@aalto.fi (A. Horton), matti.kummu@aalto.fi (M. Kummu)

HIGHLIGHTS

- We study the impact of future scenarios on floods in the Cambodian Mekong floodplain
- The full combined development scenario alters flows up to –30% in wet season and +140% in dry season
- Hydropower developments alone reduce total flood extents by more than 20%
- Prey Veng and Takeo are the provinces most susceptible to climate change induced flood risks

Style Definition: Heading 2: Indent: Left: 0 cm, Hanging: 0.95 cm, Outline numbered + Level: 1 + Numbering Style: 1, 2, 3, ... + Start at: 1 + Alignment: Left + Aligned at: 0 cm + Tab after: 1.27 cm + Indent at: 1.27 cm

Formatted: Superscript

Formatted: Outline numbered + Level: 1 + Numbering Style: Bullet + Aligned at: 0.63 cm + Indent at: 1.27 cm

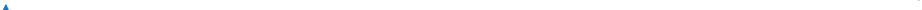
Formatted: Font color: Black

Formatted: Normal, Border: Top: (No border), Bottom: (No border), Left: (No border), Right: (No border), Between : (No border), Tab stops: 7.96 cm, Centered + 15.92 cm, Right

|

|

±
1



Formatted: Font color: Black

Formatted: Normal, Border: Top: (No border), Bottom: (No border), Left: (No border), Right: (No border), Between : (No border), Tab stops: 7.96 cm, Centered + 15.92 cm, Right

1 ABSTRACT

2 Water infrastructure development is considered necessary to drive economic growth in the
3 Mekong region of mainland Southeast Asia. Yet the current understanding of hydrological
4 and flood pattern changes associated with infrastructural development still contain several
5 knowledge gaps, such as the interactions between multiple drivers, which may have serious
6 implications for water management, agricultural production, and ecosystem services. This
7 research attempts to conduct a cumulative assessment of ~~multiple infrastructural~~
8 ~~developments~~ basin-wide hydropower dam construction and irrigation expansion, as well as
9 climate change-, implications on discharge and flood changes in the Cambodian Mekong
10 floodplain. ~~The developmental activity~~ These floodplains offer important
11 livelihoods for a considerable part of ~~hydropower dam construction and irrigation expansion,~~
12 ~~as well as climate change were considered~~ the 6.4 million people living on them, as they are
13 among the most productive ecosystems in ~~our~~ the world – driven by the annual flood
14 pulse. To assess the potential future impacts, we used an innovative combination of three
15 models: Mekong basin-wide distributed hydrological model IWRM-VMod, whole Mekong
16 delta 1D flood propagation model MIKE-11 and 2D flood duration and extent model IWRM-
17 Sub enabling detail floodplain modelling. We then ran scenarios to approximate possible
18 conditions expected by around 2050. The scenarios approximate the conditions expected by
19 around 2050. Our results show that the monthly and seasonal hydrological regimes
20 (discharges, water levels, and flood dynamics) will be subject to substantial alterations under
21 future development scenarios. ~~The degree of hydrological~~ Projected climate change impacts
22 are expected to decrease dry season flows and increase wet season flows, which is in
23 opposition to the expected alterations under ~~the combined~~ development scenarios that
24 consider both hydropower and irrigation ~~impacts are somewhat counteracted by the effect of~~
25 climate change. The likely impact of decreasing water discharge in the early wet season (up
26 to –30%) will pose a critical challenge to rice production, whereas the likely increase in water
27 discharge in the mid-dry season (up to +140%) indicates improved water availability for
28 coping with drought stresses and sustaining environmental flows. At the same time, these
29 changes would have drastic impacts on total flood extent, which is projected to decline by
30 around 20%, having potentially negative impacts on floodplain productivity and aquaculture,
31 whilst reducing the flood risk to more densely populated areas. Our findings highlight the
32 hydrological complexity and heterogeneity of this region and demonstrate the substantial

Formatted: Left, Space After: 8 pt, No bullets or numbering

Formatted

Formatted: Highlight

Formatted: Highlight

Formatted: Highlight

Formatted: Highlight

Formatted: Highlight

Formatted: Highlight

Formatted: Highlight

Formatted: Highlight

Formatted: Highlight

Formatted: Highlight

Formatted: Highlight

Formatted: Font color: Black

Formatted: Normal, Border: Top: (No border), Bottom: (No border), Left: (No border), Right: (No border), Between : (No border), Tab stops: 7.96 cm, Centered + 15.92 cm, Right

changes that planned infrastructural development will have on the area, potentially impacting important ecosystems and people's livelihoods, calling for actions to mitigate these ecologically fragile floodplains changes as well as planning potential adaptation strategies.

Formatted: Highlight

Formatted: Highlight

Keywords: Cambodian Mekong floodplain, Climate change, Cumulative impact assessment, Hydrological alteration, Hydropower dam, IWRM model

1. Introduction

The Mekong River Basin is the largest river basin in the Southeast Asian mainland. Historically, cyclones and severe tropical storms have generated the most significant Mekong flooding events, the largest of which was recorded in 1966, when tropical storm Phyllis struck the Upper Mekong Basin (Adamson et al., 2009). At the downstream end of the basin (Fig. 1), severe floods have most commonly been recorded in the area around Stung Treng Province, at the confluence of the Mekong and Tonle Sap rivers, and within the Vietnamese Mekong Delta. The last severe flood occurred in 2011 and it is ranked among the highest discharge recorded in the Lower Mekong Basin (LMB) (MRC, 2011).

Whilst prolonged flooding damages infrastructure, crops and floodplain vegetation, and the fertile land, seasonal flooding is a vital hydrological characteristic of the Mekong River Basin, as it improves water availability during the dry season, and maintains and increases the high productivity of ecosystems and biodiversity (Arias et al., 2014; Arias et al., 2012; Boretti, 2020; Kondolf et al., 2018; Kummu et al., 2010; Kummu and Sarkkula, 2008; Lamberts, 2008; Schmitt et al., 2018; Schmitt et al., 2017; Västilä et al., 2010; Ziv et al., 2012). As part of the annual flood cycle, floodwaters play an important role in the recharging of aquifers and ensuring the hydrological connectivity of the floodplain, which is essential to maintaining ground water resources for use during the dry season (Kazama et al., 2007; May et al., 2011). Floodwaters also transport essential sediments and nutrients from the river channel into the floodplain and distribute them across a wide area, fertilizing, which fertilizes agricultural lands and enhance floodplain productivity (Arias et al., 2014; Kummu and Sarkkula, 2008; Lamberts, 2008). In addition, the wider the flood extent, the larger the area of interaction between aquatic and terrestrial phases, which increases the potential transfer of floodplain terrestrial organic matter into the aquatic phase. Under the combined impacts of hydropower infrastructure and climate change, the flooded area in Cambodia's Tonle Sap Lake Basin is projected to decline by up to 11% circa 2050, which may lead to a decline in the net

Formatted: Font color: Black

Formatted: Normal, Border: Top: (No border), Bottom: (No border), Left: (No border), Right: (No border), Between : (No border), Tab stops: 7.96 cm, Centered + 15.92 cm, Right

64 sedimentation and the aquatic net primary production of up to 59%, and 38% respectively
65 (Arias et al., 2014; Lamberts, 2008).

66 Existing hydrological and flood regimes will likely be altered due to climate change
67 and infrastructure developments; but the degree of alterations vary with different drivers,
68 location, and time (Hoang et al., 2016; Hoang et al., 2019; Lauri et al., 2012; Piman et al., 2013;
69 Try et al., 2020a). Hoang et al. (2016) project that the Mekong's discharge under climate
70 change conditions by 2050 under RCP 8.5 will decrease in the wet season (up to -7%)% at
71 [Stung Treng](#) and increase in the dry season (up to +33%)% at [Chiang Saen](#), equivalent to an
72 annual increase between +5% and +15%. Lauri et al. (2012) shows that hydrological conditions
73 of the Mekong River Basin were highly dependent upon the Global Climate Model (GCM)
74 being used, with projections of water discharge at Kratie station (Fig. 1), Cambodia, ranging
75 from -11% to +15% for the wet season and from -10% to +13% for the dry season for
76 projections circa 2050. The study also concludes that the impact on water discharge due to
77 planned reservoirs was much larger than those simulated due to climate change, with water
78 discharge during the dry and early wet season being primarily determined by reservoir
79 operation. Hoang et al. (2019) find that for the same period [under RCP 8.5](#) hydropower
80 development plans in Mekong River Basin are expected to increase dry season flows up to
81 +133% and decrease wet season flows up to -16%. The future expansion of irrigated lands in
82 the wider Mekong region is expected to reduce river flows up to -9% in the driest month
83 (Hoang et al., 2019). ~~These hydrological alterations are likely to intensify when considered~~
84 ~~cumulatively.~~

85 Changes to the Mekong mainstream flows will have direct impacts on flooding in the
86 LMB floodplains in Cambodia and Vietnam. Try et al. (2020a) considered the impact of future
87 climate change (circa 2100 [under RCP 8.5](#)) in isolation on the flood dynamics of the LMB,
88 projecting an increased flood extent area of 19–43%. Infrastructure development, in contrast,
89 is expected to cause a decline in the Tonle Sap's flood extent by up to 1,200 km² (Arias et al.,
90 2012), as dam development alone is expected to reduce flooded area in the Vietnamese Mekong
91 Delta by 6% in the wet year and by 3% in the dry year (Dang et al., 2018). Flood extent in the
92 Vietnamese Mekong Delta is projected to increase by 20% under the cumulative impacts of
93 climate change and infrastructure development, bringing prolonged submergences of 1–2
94 months (Triet et al., 2020).

Formatted: Font color: Black

Formatted: Normal, Border: Top: (No border), Bottom: (No border), Left: (No border), Right: (No border), Between : (No border), Tab stops: 7.96 cm, Centered + 15.92 cm, Right

95 The impacts described above may eventually lead to a new hydrological and flood
96 regime in the Mekong region, and would likely endanger the riverine ecology and endemic
97 aquatic species of the Mekong floodplain (Arias et al., 2012; Dang et al., 2018; Kumm
98 Sarkkula, 2008; Räsänen et al., 2012). To effectively manage and overcome these pressures
99 and challenges in any floodplain, there is an urgent need to evaluate the combined impacts of
100 climate change and infrastructure operations basin-wide (Hoang et al., 2019; Hoanh et al.,
101 2010; Lauri et al., 2012; Västilä et al., 2010). However, the existing studies have focused either
102 on the basin scale flow changes (Dang et al., 2018; Hoang et al., 2016; Hoang et al., 2019;
103 Hoanh et al., 2010; Lauri et al., 2012; Pokhrel et al., 2018; Try et al., 2020a) or assessed the
104 impacts on flooding either for the Tonle Sap (Arias et al., 2012; Chen et al., 2021; Ji et al.,
105 2018; Yu et al., 2019) or the Vietnamese Mekong Delta (Dang et al., 2018; Tran et al., 2018;
106 Triet et al., 2020). Very little is known how basin-wide development and climate change would
107 impact Cambodian Mekong floodplain other than the Tonle Sap (Fig. 1), despite them being
108 important agricultural lands and home to more than 6.4 million people (2008 Population
109 Census).

110 Therefore, we have attempted to quantify the cumulative impacts of water resources
111 development plans and climate change on hydrological and flood conditions localised in the
112 Cambodian Mekong floodplain (Fig. 1) by using an innovative combination of state-of-the-art
113 hydrological and hydrodynamic models. In concentrating on the provincial level, using an
114 extended time-series for the calibration period, validating the flood extent against satellite
115 imagery, and incorporating a larger set of driving factors within our analysis, the present study
116 is a novel contribution to the work being done to understand the potential for future changes to
117 the complex hydrology of the floodplains in general, and specifically the Cambodian Mekong
118 floodplain. The results of this study may contribute to formulating adaptation and mitigation
119 strategies to flood-prone areas that balance the need for flood prevention and water resource
120 allocation against the ecological functioning of the floodplain.

121 **2. Materials and methods**

122 *2.1. Study area*

123 The study area is located in the downstream part of the Cambodian Mekong River Basin
124 (excluding the Tonle Sap Lake region), also known as the “Cambodian Mekong floodplain”
125 (Fig. 1). The area is about 27,760 km² and extends along the Mekong mainstream from Kratie

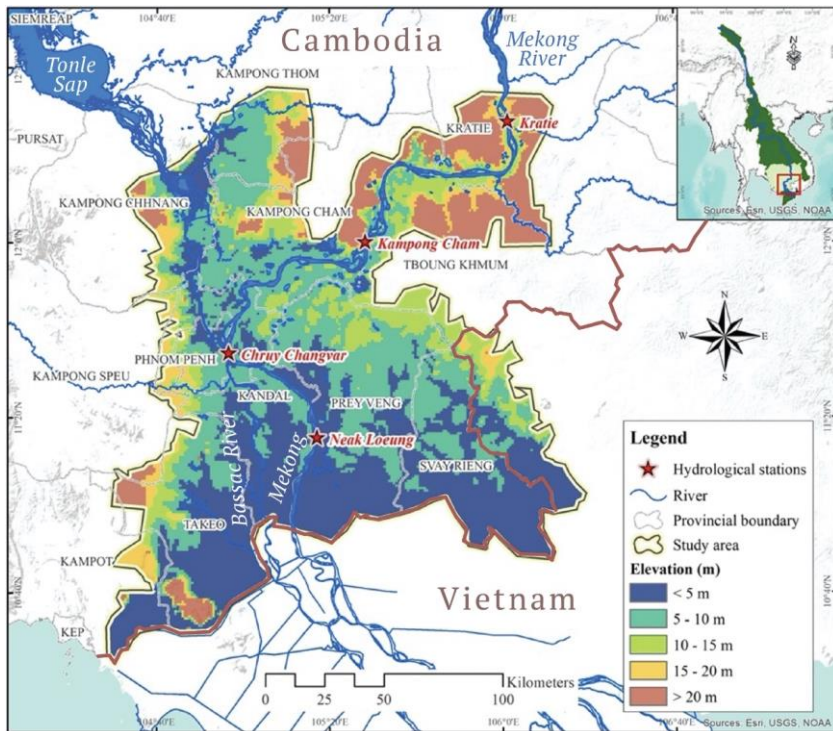
4
4

Formatted: Font color: Black
Formatted: Normal, Border: Top: (No border), Bottom: (No border), Left: (No border), Right: (No border), Between : (No border), Tab stops: 7.96 cm, Centered + 15.92 cm, Right

126 province to the Cambodia-Vietnam border. It covers parts of 12 provinces in Cambodia and
127 one province in Vietnam (Tay Ninh), but does not extend into the Vietnamese Mekong Delta
128 region (see division in Fig. 1).

129 A major part of the Cambodian Mekong floodplain is characterized by a flat terrace and
130 low-lying grounds with gentle slopes that contain many depressions and lakes, except for the
131 upper parts of the Prek Thnot and Prek Chhlong tributaries, which contains steeper terrain.
132 Hydrological conditions within the area are dominated by the seasonality and year-to-year
133 variability of the Mekong flow regimes. The wet season runs from June to October, and the dry
134 season runs from November to May. During the wet season, the characteristics of the floodplain
135 and Tonle Sap Lake play a vital role in flood peak attenuation and regulation temporarily
136 storing and later conveying water across the vast low-lying areas. During the wet season, water
137 flows from the Mekong mainstream into the Tonle Sap Lake, but this flow is then reversed in
138 the dry season. This illustrates the highly complex hydrological system at play throughout the
139 region, and the seasonal variations that characterize the ecological and agricultural landscape.

140 Within our historic baseline period of 1971–2000, the annual average temperature
141 across the study area varies from 26.9°C to 28.2°C, with mean monthly temperatures between
142 30°C during the hottest months (April and/or May), and 26°C in the coldest month (January).
143 Average annual rainfall across the study area during the same period varies between 1,100 mm
144 and 1,850 mm, with mean monthly rainfall ranging between 250 mm in the wettest months
145 (May/June), and 10 mm in the driest (February).



Formatted: Font color: Black

Formatted: Normal, Border: Top: (No border), Bottom: (No border), Left: (No border), Right: (No border), Between : (No border), Tab stops: 7.96 cm, Centered + 15.92 cm, Right

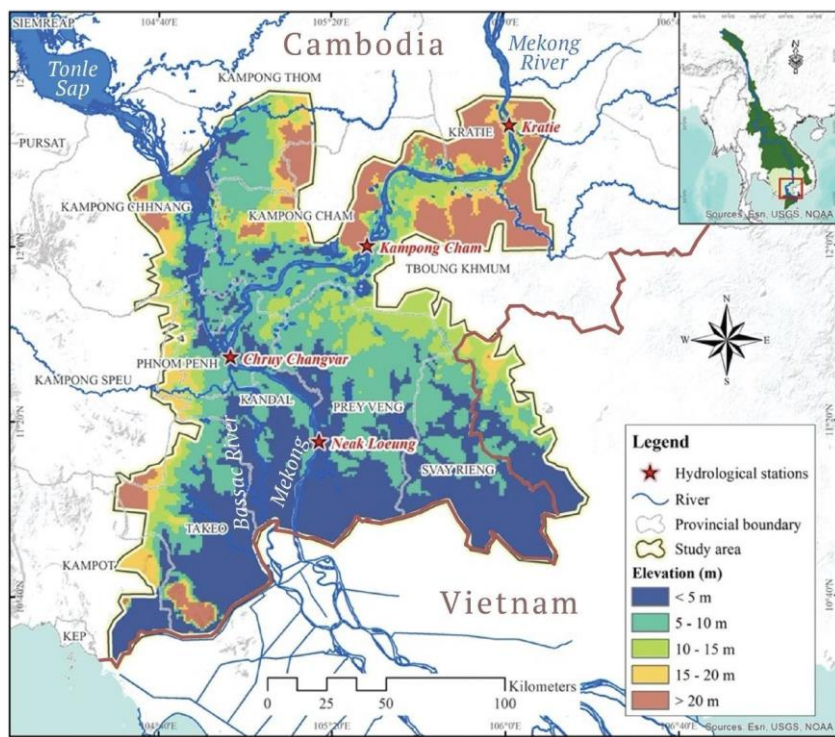


Fig. 1. Map of the study area, the Cambodian Mekong floodplain. Elevation of 90-m grid cell was extracted from the SRTM database and river lines were obtained from the MRC database.

2.2. Modelling structure and datasets

We used a hydrological – floodplain model combination (Fig. 2), consisting of the distributed hydrological model IWRM-VMod (Lauri et al., 2006), the floodplain propagation model MIKE 11 (Dung et al., 2011), and the flood extent and duration model IWRM-Sub (MRC, 2018a) (Fig. 2). First, the IWRM-VMod model with resolution of 5 km x 5 km (see extent and hydrological processes in Fig. 2a) was used to simulate the entire Mekong basin's flow response to hydropower developments, irrigation expansion, and climate change impacts at around year 2050. We used the model runs, both baseline and scenarios, from Hoang et al. (2019). From the hydrological model we derived the boundary condition discharges that were used to drive the 1D flood propagation model MIKE 11 (as constructed and employed in Triet et al., 2017, 2020) in order to obtain the initial floodplain conditions, water levels, and fluctuating discharge of the Tonle Sap River. MIKE 11 model extends over the entire Mekong Delta down to the South China Sea, where sea level is used as another boundary

Formatted: Font color: Black

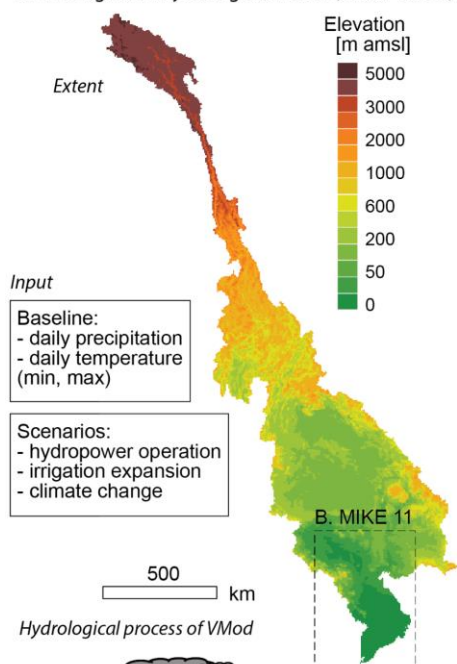
Formatted: Normal, Border: Top: (No border), Bottom: (No border), Left: (No border), Right: (No border), Between : (No border), Tab stops: 7.96 cm, Centered + 15.92 cm, Right

163 condition. MIKE 11 also includes a detailed description of the channels, canals, and sluice
164 gates in the delta (Triet et al 2020). The results from MIKE 11 in turn were used as boundary
165 conditions to the detail scale (1 km x 1 km) floodplain hydrodynamic IWRM-Sub model. The
166 IWRM-Sub model is a flood model that also has hydrological processes (i.e., precipitation,
167 evaporation, etc) in it, making it ideal for large floodplain modelling in monsoon climate. It
168 uses the 2D depth averaged Navier Stokes, and St Venant equations to propagate a flood
169 wave out into the floodplain from the water level points passed as boundary conditions
170 (MRC, 2018a).

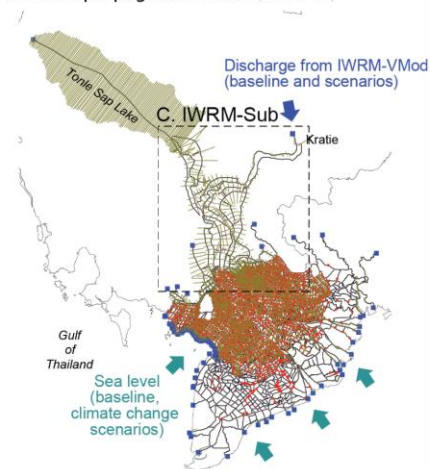
171 The IWRM-Sub model was applied to Cambodian floodplains for the Mekong River
172 Commission's (MRC) Council Study (MRC, 2018a). It is based on the SRTM 90-m
173 topographical map (Jarvis et al., 2008), a soil types map (FAO, 2003), and a land use map
174 (GLC2000, 2003), all aggregated to 1 km × 1 km resolution (Table 1). Geospatial data and
175 river cross-section data were retrieved and added from the Mekong River Commission
176 (MRC). The future climate scenarios are based on an ensemble of 5 GCM projections of
177 precipitation and temperature taken from the CMIP5 suite of models (ACCESS, CCSM,
178 CSIRO, HadGEM2, and MPI). Whilst the CMIP6 collection has now superseded the CMIP5
179 model results, an analysis of the differences between model collections shows consistent
180 mean values for both precipitation and temperature across our study area for both wet and dry
181 seasons (Table S1).

Formatted: Font color: Black
Formatted: Normal, Border: Top: (No border), Bottom: (No border), Left: (No border), Right: (No border), Between : (No border), Tab stops: 7.96 cm, Centered + 15.92 cm, Right

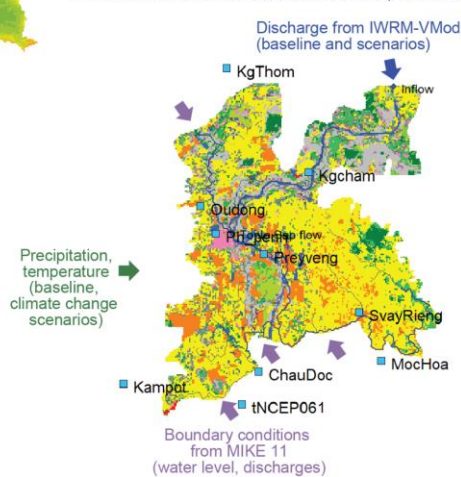
A. Mekong basin hydrological model (IWRM-VMod)



B. Flood propagation model (MIKE 11)



C. Flood extent and duration model (IWRM-Sub)



Formatted: Font color: Black

Formatted: Normal, Border: Top: (No border), Bottom: (No border), Left: (No border), Right: (No border), Between : (No border), Tab stops: 7.96 cm, Centered + 15.92 cm, Right

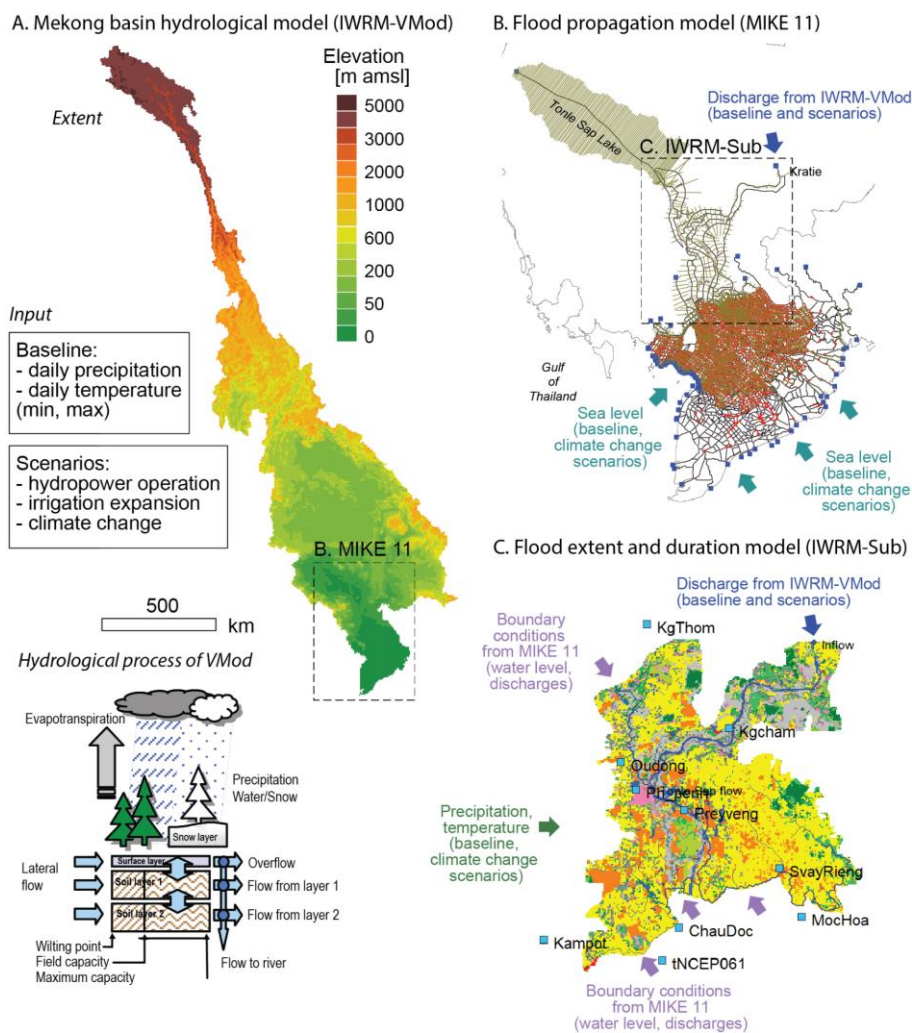


Fig. 2. Schematic illustration of the modelling setup. A: Mekong basin hydrological model IWRM-VMod models the hydrology of the entire Mekong basin with 5 km x 5 km resolution (Hoang et al 2019). B: Flood propagation model MIKE 11 models the hydrodynamics of the entire Mekong floodplain using the discharges from IWRM-VMod and sea level in South China Sea as boundary conditions (Triet et al, 2017). C: Flood extent and duration model IWRM-Sub is a detailed 2D floodplain model using the output from two other models as an input.

Flood extent maps for calibration and validation were derived from Landsat images using a sophisticated water detection algorithm developed and optimized for the Lower Mekong region (Donchyts et al., 2016). All IWRM-Sub model inputs and their brief description are

Formatted: Font color: Black

Formatted: Normal, Border: Top: (No border), Bottom: (No border), Left: (No border), Right: (No border), Between : (No border), Tab stops: 7.96 cm, Centered + 15.92 cm, Right

presented in Table 1, while input data for IWRM-VMod is detailed in Hoang et al (2019) and MIKE 11 in Triet et al. (2020).

Table 1. List and brief description of datasets for IWRM-Sub.

No.	Data type	Period	Resolution	Source
1	Topography (digital elevation model)	–	90 m	Shuttle Radar Topography Mission 2000
2	Land use map	2003	1 km	Global Land Cover 2000
3	Soil types map	2003	1 km	Food and Agriculture Organization
4	Meteorological data <ul style="list-style-type: none"> • Temperature • Rainfall 	1971–2000	Daily	Ensemble of 5 GCMs (ACCESS, CCSM, CSIRO, HadGEM2, and MPI)
5	Historical discharge data	1985–2000	Daily	Mekong River Commission
6	Historical water level data	1985–2000	Daily	Mekong River Commission
7	Hydropower dams and irrigation	–	–	Mekong River Commission
8	Climate change projections of temperature and precipitation.	2036–2065	Daily	Ensemble of 5 GCMs (ACCESS, CCSM, CSIRO, HadGEM2, and MPI)
9	Flood extent maps (satellite image)	1985–2008	30 m	SERVIR-Mekong
10	River cross-section	–	–	Mekong River Commission

Formatted: Indent: Left: 0 cm, Hanging: 0.45 cm, Outline numbered + Level: 1 + Numbering Style: Bullet + Aligned at: 0.63 cm + Indent at: 1.27 cm

2.3. Modelling methodology

We adapted and applied the existing IWRM-VMod (Hoang et al., 2019), MIKE11 (Triet et al., 2017), and IWRM-Sub (MRC, 2018a) models to assess the smaller scale cumulative impacts of future development plans and climate change on the Cambodian Mekong floodplain. Here we enhanced the reliability of these existing models, particularly in the Cambodian Mekong floodplain, by advancing the predictive accuracy of the hydrology (recalibration), accounting for multiple calibration stations (four stations), and validating flood extents against satellite imagery, as described below.

Formatted: Font color: Black

Formatted: Normal, Border: Top: (No border), Bottom: (No border), Left: (No border), Right: (No border), Between : (No border), Tab stops: 7.96 cm, Centered + 15.92 cm, Right

Our initial model setup describes the current state of the floodplain for the historic baseline period of 1971–2000, which we further calibrated and validated against observations of water discharge and water level taken at Kratie, Kampong Cham, Chroy Changvar, and Neak Loeung hydrological stations (see locations in Fig. 1). The model performance was systematically quantified and evaluated based upon the Nash-Sutcliffe efficiency (NSE), percent bias (PBIAS), ratio of the root mean square error to the standard deviation of observed data (RSR), and coefficient of determination (R^2).

The use of 1971-2000 as our baseline represents well the hydrological state of the basin before major alterations were introduced (Soukhaphon et al., 2021). Including years after 2000 in our baseline would introduce significant hydrological and irrigation influences that would prohibit a thorough examination of these in isolation as part of our simulations.

Flood extent maps generated from the IWRM-Sub model were validated for the same period against satellite-based flood extent maps generated by the Surface Water Mapping Tool (SWMT). The SWMT is a Google Appspot based online application developed by Donchyts et al. (2016). A stack of Landsat (4 and 5) data were generated using SWMT from 1984 - 2000. This stack of images was then used to generate a water index map using the Modified Normalized Difference Water Index (MNDWI) (Xu, 2006) to distinguish between water and non-water areas, which were then adjusted to account for dark vegetation and hill shadows using a Height Above Nearest Drainage (HAND) map (Rennó et al., 2008). Fig. S1 illustrates all procedures of the Surface Water Mapping Tool.

To evaluate the model performance for flood inundation maps, we applied three indices: Recall, Precision, and the ratio between simulated and observed flood extent areas. Recall evaluates what proportion (0-1) of the flood derived from remote sensing images are identified by the simulation. Precision evaluates what proportion of the simulated extent agrees with the remote sensing data. If the simulated extent overlaps the observed extent area perfectly, recall, precision, and the ratio of extents become 1.

Once the IWRM-Sub model was successfully calibrated and validated, we modulated the inflow at Kratie and at the confluence of the Tonle Sap River with the main Mekong channel to represent the upstream impacts of multiple development and climate change scenarios (see Section 2.4). We then simulated the Cambodian Mekong floodplain’s hydrological and flood conditions (flood extent, flood depth, and flood duration) for each scenario.

Formatted: Font color: Black

Formatted: Normal, Border: Top: (No border), Bottom: (No border), Left: (No border), Right: (No border), Between : (No border), Tab stops: 7.96 cm, Centered + 15.92 cm, Right

236 2.4. Analytical scenario descriptions

237 The scenario setup that we adopted for our study is the same as that described in Hoang et al.
238 (2019). The baseline (1971-2000) represents the Mekong basin at a time before significant
239 alterations to the hydrological functioning of the catchment have occurred through
240 infrastructural development. We then defined 11 development scenarios that cover each of the
241 three main drivers of hydrological change in isolation (hydropower, irrigation, and climate
242 change), as well as combinations of these together. For future scenarios, we used climate data
243 from an ensemble of five GCMs (ACCESS, CCSM, CSIRO, HadGEM2, and MPI) for the
244 years 2036-2065, and considered representative concentration pathway (RCP) levels 4.5 and
245 8.5. [These GCMs were selected based on their performance in reproducing historic
246 temperature, seasonal precipitation, and climate extremes in the Mekong region. The GCM
247 data were downscaled using bilinear interpolation and statistically bias corrected using a
248 quantile mapping method. For full details see Hoang et al \(2016; 2019\). The sea level boundary
249 condition was adjusted by 43 cm for future scenarios to account for the combined effects of
250 sea level rise and deltaic subsidence, taken as the average of the range estimated by Manh et al
251 \(2015\) i.e., 22-63 cm. This value was used for both RCP4.5 and RCP8.5 as the climate change
252 component of sea level rise for our study period taken from IPCC \(2014\) is relatively consistent
253 across RCP scenarios \(RCP4.5: 19-33 cm; RCP8.5: 22-38 cm\).](#) Our hydropower development
254 scenario includes 126 dams on both mainstems (N= 16) and tributaries (N= 110) of the
255 Mekong, equivalent to a total active storage of 108 km³, all of which are planned to be active
256 between 2036 and 2065. [Dam simulation was based on the optimisation scheme developed by
257 Lauri et al. \(2012\), which calculates each dam's operating rules separately in a cascade, aiming
258 to maximise productive outflows \(i.e., outflows through the turbines\), thus maximising hydro-
259 power production.](#) We included two irrigation scenarios, a high and low expansion version,
260 using the global projected irrigation expansion scenarios by Fischer et al. (2007) applied to the
261 baseline irrigation extent taken from the MIRCA - 'Global Dataset of Monthly Irrigated and
262 Rain-fed Crop Areas around the Year 2000' (Portmann et al., 2010). A list of scenarios and
263 their notation are presented in Table 2, and a thorough description and justification for these
264 scenarios can be found in Hoang et al. (2019).

265

266

Formatted: Font color: Black

Formatted: Normal, Border: Top: (No border), Bottom: (No border), Left: (No border), Right: (No border), Between : (No border), Tab stops: 7.96 cm, Centered + 15.92 cm, Right

267 **Table 2.** Summary of scenario names, driving climate data, and development inclusion
268 descriptions. [See Section 2.4 for data description.](#)

Scenario name	Scenario description		
	Climate data	Hydropower	Irrigation
S1_Baseline	Baseline (1971 - 2000)	Circa 2000	Circa 2000
S2_Hydropower	Baseline (1971 - 2000)	Future development	Circa 2000
S3_Irrigation_High	Baseline (1971 - 2000)	Circa 2000	HIGH irrigation expansion
S4_Irrigation_Low	Baseline (1971 - 2000)	Circa 2000	LOW irrigation expansion
S5_CC_RCP45	Future (2036 - 2065) RCP 4.5	Circa 2000	Circa 2000
S6_CC_RCP85	Future (2036 - 2065) RCP 8.5	Circa 2000	Circa 2000
S7_HP_RCP45	Future (2036 - 2065) RCP 4.5	Future development	Circa 2000
S8_HP_RCP85	Future (2036 - 2065) RCP 8.5	Future development	Circa 2000
S9_LI_HP_RCP45	Future (2036 - 2065) RCP 4.5	Future development	LOW irrigation expansion
S10_LI_HP_RCP85	Future (2036 - 2065) RCP 8.5	Future development	LOW irrigation expansion
S11_HI_HP_RCP45	Future (2036 - 2065) RCP 4.5	Future development	HIGH irrigation expansion
S12_HI_HP_RCP85	Future (2036 - 2065) RCP 8.5	Future development	HIGH irrigation expansion

269

270 **3. Results**

271 *3.1. Predictive accuracy of the models*

272 The Mekong basin wide IWRM-VMod hydrological model was calibrated and validated
273 against discharges in various stations, with very good performance: validation period NSE at
274 Nakhon Phanom station of 0.74, and at Stung Treng station of 0.64 (Hoang et al., 2019). MIKE

14
14

Formatted Table

Formatted Table

Formatted: Font color: Black

Formatted: Normal, Border: Top: (No border), Bottom: (No border), Left: (No border), Right: (No border), Between : (No border), Tab stops: 7.96 cm, Centered + 15.92 cm, Right

11 model application to the entire Mekong delta was, in turn, validated against two flood events in 2000 and 2011 in Triet et al (2017) also with good correspondence to the observations achieving NSE to observed water levels of between 0.72 and 0.97 across 19 different gauging stations.

Here we validated the IWRM-Sub model for Cambodian Mekong floodplain against water levels and discharge in four stations and flood extent based on Landsat imagery (see Methods). Based on the validation measures (Table 3), a good model performance is obtained at all stations (both water discharge and water level) with the values of NSE between 0.69 and 0.87, PBIAS between -14.4% and +9.8%, RSR between 0.37 and 0.55, and R^2 between 0.89 and 0.93. It should be noted that the statistical model performance with NSE and R^2 greater than 0.5, PBIAS between $\pm 25\%$, and RSR less than 0.7 is indicated as decision guidelines for hydrologic model studies (Benaman et al., 2005; Setegn et al., 2010). A time series comparison between the simulated and observed water discharge and water level (1985–2000) at four hydrological stations can be found in Fig. S2 and Fig. S3. It is apparent that the simulated water discharge among these stations is well in line with the observed data throughout the 15-year hydrological record available for comparison.

Results of the flood extent comparison between IWRM-Sub model and SWMT observations over the time horizon 1985–2000 show equally a good agreement. The model underestimates the total flooded area by just 0.1% as the ratio of simulated to observed flooded extent areas is 0.99. However, the overlapping flooded area only constituted 71% of the observed (SWMT) extent (which constitutes the recall), and 72% of the simulated (IWRM-sub) extent (which is the precision) (Fig. 3). Part of this discrepancy may be accounted for by the inclusion of rivers and lakes in the extent of the simulation, yet not in the SWMT derived extents. -Using multiple models in succession can have the negative effect of compounding errors, however these results demonstrate that this has not unduly impacted our methodology as our estimations closely match the observations of flood extent.

Table 3. ~~Statistical model~~Model performance at four hydrological stations (1985–2000) ~~evaluated with daily values.~~ See station locations in Fig. 1. Note: the statistical model performance with Nash Sutcliffe Efficiency (NSE) and the coefficient of determination (R^2) greater than 0.5, percentage bias (PBIAS) between $\pm 25\%$, and the ratio of the root mean square error to the standard deviation (RSR) less than 0.7 is indicated as decision guidelines for hydrologic model studies (Benaman et al., 2005; Setegn et al., 2010).

Formatted: Font color: Black
Formatted: Normal, Border: Top: (No border), Bottom: (No border), Left: (No border), Right: (No border), Between : (No border), Tab stops: 7.96 cm, Centered + 15.92 cm, Right

|

|

Station	Water discharge				Water level			
	NSE	PBIAS (%)	RSR	R ²	NSE	PBIAS (%)	RSR	R ²
Kratie	0.79	0.9	0.45	0.89	0.69	−14.4	0.55	0.93
Kampong Cham	0.80	4.5	0.45	0.90	0.87	-1.4	0.37	0.93
Chroy Changvar	0.80	9.8	0.45	0.91	0.86	-3.4	0.37	0.93
Neak Loeung	0.81	-5.6	0.44	0.91	0.85	3.8	0.38	0.93

Formatted Table

|

Formatted: Font color: Black

Formatted: Normal, Border: Top: (No border), Bottom: (No border), Left: (No border), Right: (No border), Between : (No border), Tab stops: 7.96 cm, Centered + 15.92 cm, Right

308
309

310
311
312
313
314
315
316
317
318
319

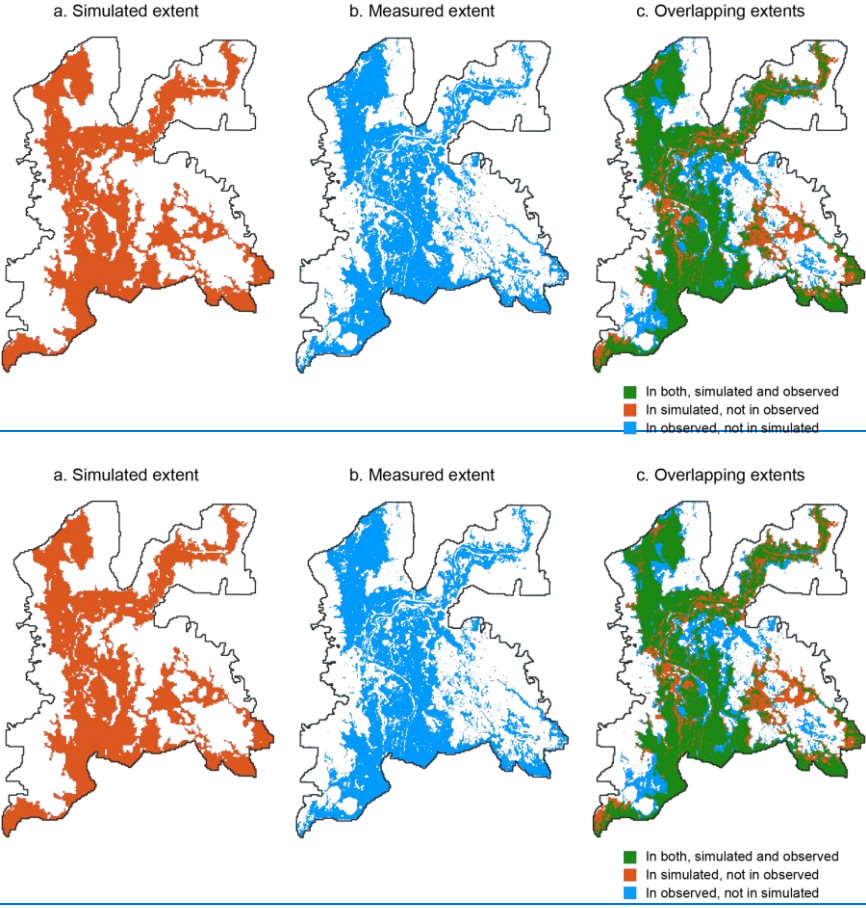


Fig. 3. Comparison of maximum flood extent resulting from the model and measured from satellite images.

3.2. Impacts on hydrological conditions

Having run the model for each of the development scenarios (S1-S12; see Table 2), we obtained the corresponding daily time series of water discharge and water level at each station and compared them with the baseline scenario. We then calculated the mean monthly water discharge and water level across the study period. Finally, we computed the percentage change in mean monthly water discharge and water level for each scenario at each station. The results at Kratie, Kampong Cham, and Chroy Changvar were virtually indistinguishable from one

Formatted: Font color: Black
Formatted: Normal, Border: Top: (No border), Bottom: (No border), Left: (No border), Right: (No border), Between : (No border), Tab stops: 7.96 cm, Centered + 15.92 cm, Right

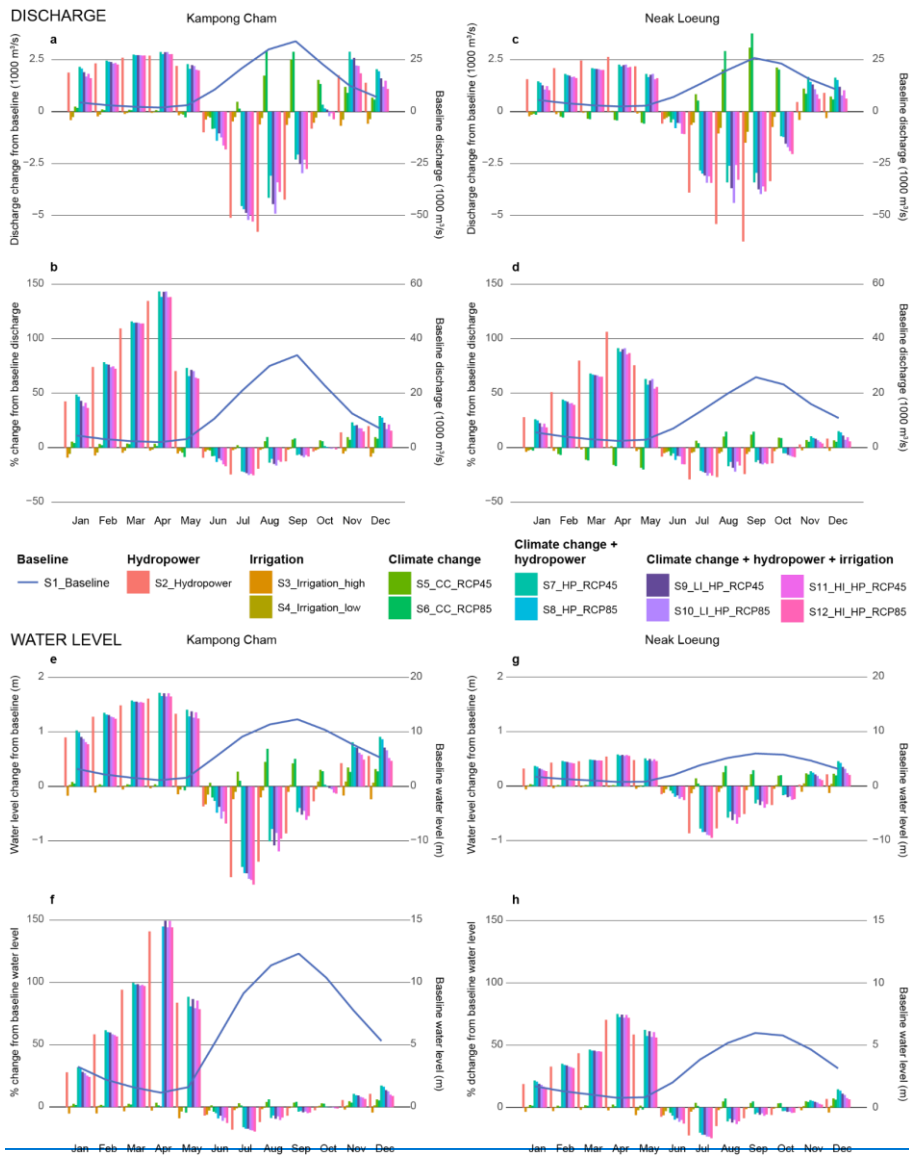
another, so to avoid unnecessary repetition, we have presented results from only Kampong Cham (as the midway station) and Neak Loeung, which differs significantly from the other stations for being downstream of the Tonle Sap River confluence (Fig. 1), and the Bassac River distributary (Fig. 4).

All scenarios that contain an element of hydropower development follow the same pattern of increasing both water discharge and water level during the dry season (Nov–May), whilst reducing water discharge and water level during the early and mid- wet season (Jun–Sep) (Fig. 4). The impact of climate change appears to fluctuate during the months of January to June between Kampong Cham (and Kratie and Chruy Changvar) and Neak Loeung, as there is a slight increase in discharge and water levels at the upstream stations, yet a slight decrease at the downstream station, though the magnitude of any alteration is only small. From July to December, however, the climate change impact is much stronger and increases discharge and water levels at all stations. The larger magnitude of the climate change impacts during the wetter months counteracts the impact of hydropower and irrigation (which slightly reduces flows and water levels in all months), which can be seen in the difference between scenario S2 (hydropower solo) and scenarios S7-S12 that incorporate multiple drivers (Fig. 4; scenario description in Table 2). This is most evident at Kampong Cham station in October, where climate change impacts are large enough to offset hydropower impacts, so that only those scenarios that incorporate the additional impact of irrigation are strong enough to reduce flows and water levels. Whilst the largest magnitude impacts are in the wetter months of July to September, the proportional impacts are far larger in the dry season, where the impact of hydropower development dominate the flow regime and increase water levels up to 150% in April at Kampong Cham, compared to a maximum decrease of <25% in July.

Comparing results from upstream stations with those at Neak Loeung, we see that the magnitude of climate change impacts are larger downstream both absolutely and proportionally. This is evident in the greater differences between the solo hydropower scenario (S2) and the combined hydropower and climate change scenarios (S7-S12) here than observed at the upstream stations. Nevertheless, hydropower impacts still dominate the flow regime, especially during the drier months where discharges increase >100% in April.

Our results suggest that planned hydropower developments will drastically alter the hydrology of the Mekong main channel and far outweigh the effects of irrigation or climate change impacts in either counteracting or enhancing these alterations.

Formatted: Font color: Black
Formatted: Normal, Border: Top: (No border), Bottom: (No border), Left: (No border), Right: (No border), Between : (No border), Tab stops: 7.96 cm, Centered + 15.92 cm, Right



Formatted: Font color: Black

Formatted: Normal, Border: Top: (No border), Bottom: (No border), Left: (No border), Right: (No border), Between : (No border), Tab stops: 7.96 cm, Centered + 15.92 cm, Right

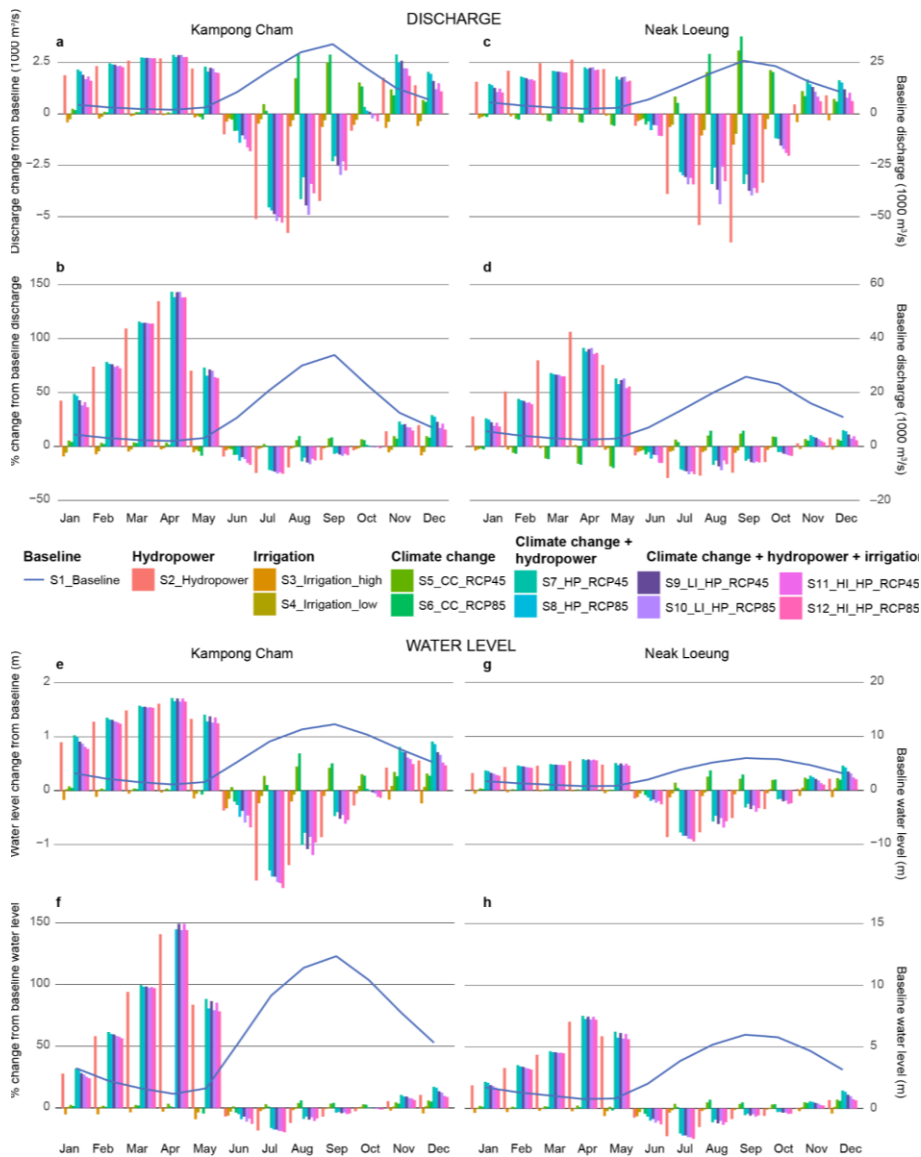


Fig. 4. Changes in monthly water discharge and water level at Kampong Cham (left hand side) and Neak Loeung (right hand side); the blue line indicates the baseline monthly discharge and water level, and the colour bar charts indicate both the magnitude (a, c, e, g) and the percentage (b, d, f, h) change under different scenarios in comparison with the baseline (1971–2000). (See location of stations in Fig. 1).

Formatted: Font color: Black

Formatted: Normal, Border: Top: (No border), Bottom: (No border), Left: (No border), Right: (No border), Between : (No border), Tab stops: 7.96 cm, Centered + 15.92 cm, Right

359 3.3. Impacts on flood conditions

360 Here we present the quantitative results together with the spatial analysis of flood conditions
361 throughout the entire study area. The comparisons between each scenario and their
362 justifications are described in the analysis at the provincial level because of the similarity in
363 patterns. Under the baseline scenario (S1), the modelling results between 1971 and 2000 show
364 that the yearly flooded area ranges from 7,785 to 11,525 km². Its mean annual value is
365 estimated at 9,370 km², about 34% of the whole study area.

366 We compared year to year the impact of each development scenario against the
367 S1_baseline (1971-2000) on the total flooded area across the study area (Fig. 5). Scenarios S2-
368 S4 use the same driving climate data as the baseline scenario (S1), and so the variability in the
369 impact shown is significantly reduced to produce consistent impacts for all years. Whereas
370 scenarios S5-S12 are driven by future climate data projections, so that the variability in
371 comparing year to year is significant. Nevertheless, there is a clear pattern that emerges once
372 again showing the dominance of hydropower development in significantly reducing the yearly
373 flooded area. The impacts of both irrigation development scenarios (S3 and S4) also reduce the
374 yearly flooded area, though to a lesser extent. Climate change impacts in isolation (S5 and S6)
375 increase the flooded area overall, though there are some years in which the area is reduced
376 compared to the baseline. The proportional magnitude of these effects is most evident in the
377 solo hydropower development with a median reduction of >20% year on year, yet the combined
378 impact of irrigation, hydropower, and climate change did reduce flooded areas by up to 40%
379 in some years (Fig. 5).

380

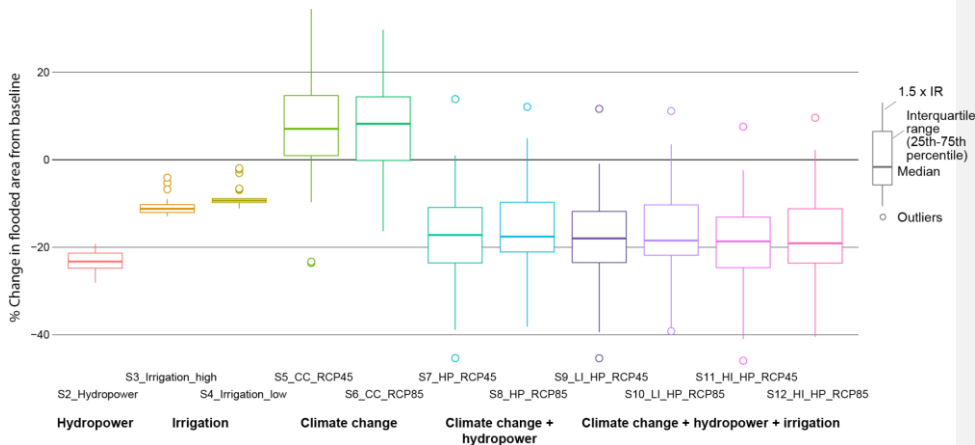
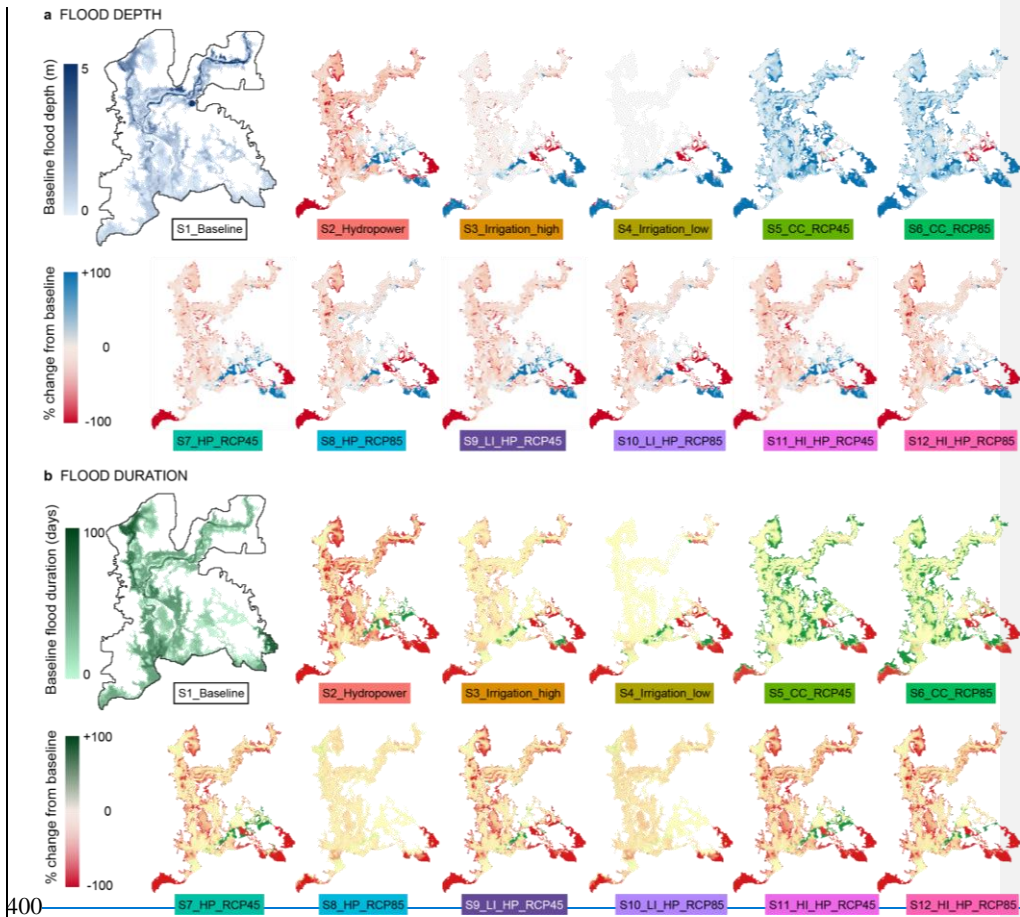


Fig. 5. Changes in total flooded area compared to the baseline period 1971–2000; the graph shows the range of changes due to interannual variation (box and whiskers), the median change (horizontal line) and outliers that were exceptional years (circles).

The spatial distribution of flood inundation and depth across the Cambodian Mekong floodplain varies greatly between scenarios of planned developments and climate change (Fig. 6). The floodplain is characterized spatially by a high fluctuation of flood depth and flood duration alteration of over $\pm 100\%$ in almost all scenarios, especially in the Southeast and the Southwest part of the study area. Whilst the magnitude of these fluctuations is large across all scenarios, it is most evident in hydropower (S2) (reductions of depth and duration) and climate change RCP 8.5 (S6) scenarios (increase in depth and duration). Though even in these most extreme cases, there are areas that run contrary to the general pattern of change, highlighting the hydrological complexity of the region. The low irrigation scenario (S4) has the least impact (Fig. 6), though even this level of development may significantly impact the lower lying regions in the southwest and southeast where much of the rice cultivation is concentrated. Our results suggest that all scenarios will cause heterogeneous impacts across the region that may effectively shift flood impacts from one area to another rather than completely dispel the associated risks.

Formatted: Font color: Black

Formatted: Normal, Border: Top: (No border), Bottom: (No border), Left: (No border), Right: (No border), Between : (No border), Tab stops: 7.96 cm, Centered + 15.92 cm, Right



Formatted: Font color: Black

Formatted: Normal, Border: Top: (No border), Bottom: (No border), Left: (No border), Right: (No border), Between : (No border), Tab stops: 7.96 cm, Centered + 15.92 cm, Right

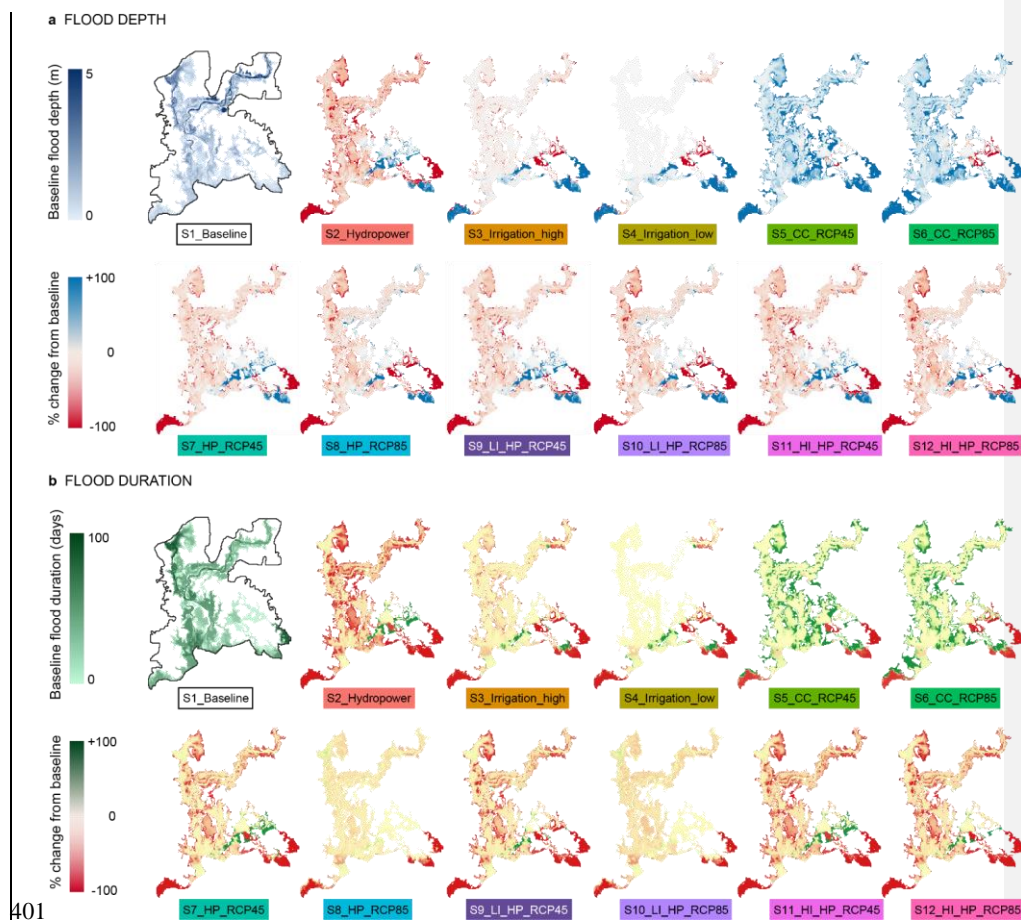


Fig. 6. Spatial distribution of changes in flood depth and duration. a: food depth; b: flood duration. Results are shown over the baseline period 1971-2000, and all scenarios (see description in Table 2).

3.4. Provincial level analysis

We examined the change in flooded area, flood depth and flood duration for 10 provinces that have a considerable part of their area within the study area (Kampong Speu and Kampot province, and Tay Ninh province in Vietnam, were not included; see Fig. 1). Each scenario was compared to the baseline period at the provincial level (Fig. 7). Under the baseline scenario (S1), the modelling results show that the average flooded area ranges from a minimum of 188 km² in Phnom Penh province to a maximum of 2,308 km² in Prey Veng province, which represents 43% of the provincial territory. Whilst the average flood depth ranges from 0.54 m in Svay Rieng province to 2.4 m in Kratie province, and the average flood duration

Formatted: Font color: Black

Formatted: Normal, Border: Top: (No border), Bottom: (No border), Left: (No border), Right: (No border), Between : (No border), Tab stops: 7.96 cm, Centered + 15.92 cm, Right

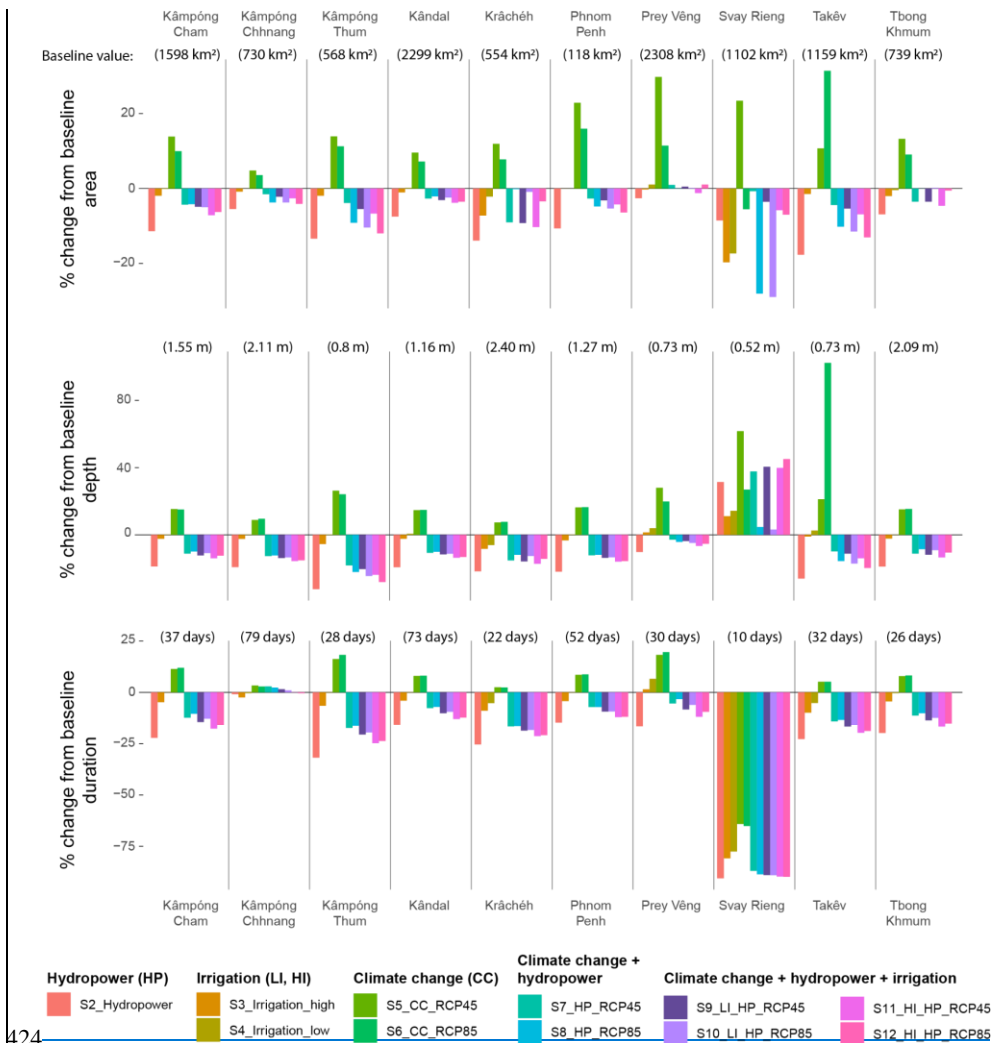
413 ranges from 10 days in Svay Rieng province to 79 days in ~~Kâmpóng~~Kampong Chhnang
414 province.

415 Except for the Svay Rieng region, which appears anomalous, ~~Kâmpóng~~Kampong
416 Chhnang and ~~Kràchéh~~Kratie are least affected by the impacts of climate change, whilst Prey
417 Veng and ~~Takev~~Takeo are most affected (Fig. 7). The development scenarios have least effect
418 in Prey Veng, where flood area and depths are almost unaffected in comparison to the other
419 provinces.

420 Svay Rieng displays an extreme reduction in flood duration for all scenarios, including
421 climate change scenarios, which is also true of the flooded area except for the RCP 4.5 climate
422 impact scenario (S5). Depths, however, increase in all scenarios suggesting that flooding in this
423 province is reduced in extent and duration to a shorter more intense (and so deep) flood event.

Formatted: Font color: Black

Formatted: Normal, Border: Top: (No border), Bottom:
(No border), Left: (No border), Right: (No border),
Between : (No border), Tab stops: 7.96 cm, Centered +
15.92 cm, Right



424

Formatted: Font color: Black

Formatted: Normal, Border: Top: (No border), Bottom: (No border), Left: (No border), Right: (No border), Between : (No border), Tab stops: 7.96 cm, Centered + 15.92 cm, Right

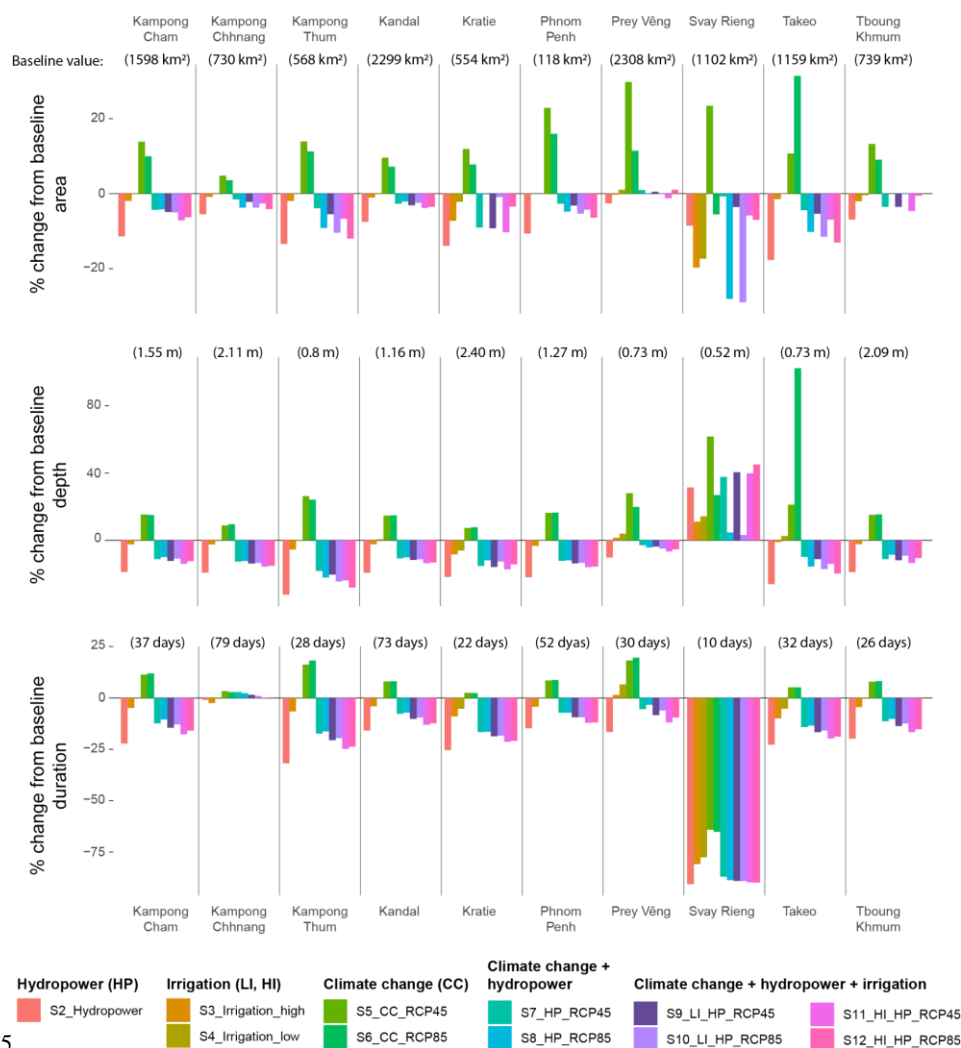


Fig. 7. Changes in annual mean flooded area, flood depth, and flood duration compared to the baseline period (1971–2000) for all scenarios at the provincial level. See province location in Fig. 1.

4. Discussion

4.1. Key findings

The model performance metrics achieved by our hydrological simulation of water discharge and water level for the baseline period of 1971–2000 at all four monitoring stations (Kratie,

Formatted: Font color: Black

Formatted: Normal, Border: Top: (No border), Bottom: (No border), Left: (No border), Right: (No border), Between : (No border), Tab stops: 7.96 cm, Centered + 15.92 cm, Right

433 Kampong Cham, Chroy Changvar and Neak Loeung) exceed existing studies within the same
434 region (Hoang et al., 2016; Hoang et al., 2019; Västilä et al., 2010), with the exception of Dang
435 et al. (2018), who recorded an NSE value of 0.98 compared to our value of 0.80 at Kampong
436 Cham station. Whilst there are studies of flood extent within our study area that only focus on
437 a single event rather than a multi-year analysis that slightly surpass our own in terms of
438 performance metrics (Fujii et al., 2003), our continual analysis of annual flood patterns
439 comprising a 30-year time horizon is comparable to, and often exceeds, other such multi-year
440 analyses done in the region (Try et al., 2020a; Try et al., 2020b). The relative success of our
441 baseline simulations allows us to have a high degree of confidence in our future projections of
442 the Cambodian Mekong floodplain's hydrological response to planned infrastructural
443 development and future climate changes. All future projections of scenarios containing
444 multiple drivers that we considered within our analysis followed the same generic pattern of
445 alterations to both the expected discharge and river water level, increasing during the dry
446 season (Nov–May), and decreasing during the early- and mid- wet season (Jun–Sep). Such a
447 general pattern of alteration is due to the overwhelming dominance of the hydropower
448 development impacts, that overcome any counteraction that might be applied by either
449 irrigation development schemes (counteracts in dry season) or climate change impacts.

450 These general trends are in line with the majority of previous research in the region
451 (Dang et al., 2018; Hoang et al., 2016; Hoang et al., 2019; Kallio and Kumm, 2021; Lauri et
452 al., 2012; Piman et al., 2013; Räsänen et al., 2012; Västilä et al., 2010). The degree of alteration
453 to these hydrological indicators is most pronounced in the upstream areas of Kratie, Kampong
454 Cham, and Chroy Changvar stations and diminishes downstream of the confluence with the
455 Tonle Sap River towards Neak Loeung station, which is also consistent with earlier findings
456 (Dang et al., 2018).

457 Our findings clearly demonstrate the homogenizing effect that the planned hydropower
458 developments would have on the Mekong River's hydrograph, which would go far beyond
459 simply contracting the impacts of other drivers and would reshape the expected flow regime,
460 massively increasing dry season low flows and significantly reducing wet season high flows.

461 The future projections of flood conditions suggest that most provinces will see an
462 increase in depth, duration, and area under climate change scenarios, but that these alterations
463 are counteracted by the combined development scenarios reflecting the flood prevention
464 benefit afforded by irrigation and hydropower scenarios. These findings are supported by other

Formatted: Font color: Black

Formatted: Normal, Border: Top: (No border), Bottom: (No border), Left: (No border), Right: (No border), Between : (No border), Tab stops: 7.96 cm, Centered + 15.92 cm, Right

465 studies that look at the impact of isolated drivers of hydrological change in the region (Fujii et
466 al., 2003; Try et al., 2020a), and studies that look at multiple drivers in nearby regions (Hoanh,
467 et al., 2010; Pokhrel et al., 2018;).

468 Our provincial level assessment shows that Prey Veng province is most vulnerable to
469 the largest flooded area (Fig. 7), as its large territory is entirely located in the low-lying area
470 adjacent to the Mekong River. Kampong Thom province receives the largest flood prevention
471 benefit provided by the planned hydropower developments, whilst Kampong Chhnang receives
472 the least in terms of flooded area and flood duration, most likely because the flood regime is
473 strongly controlled by the Tonle Sap Lake System and receives less influence from the
474 upstream flow alterations. Svay Rieng province is drastically impacted by all the scenarios.
475 This is most likely due to the extremely low ground surface elevation (majority less than 8 m)
476 meaning that slight alterations have proportionally large impacts. The region may also be
477 affected by changes to the hydrological conditions on the Vietnamese Mekong Delta, some of
478 which were represented in this study by means of the boundary conditions supplied by Triet et
479 al (2020) that considered the whole delta region.

480 *4.2. Implications of hydrological and flood condition changes*

481 Changes in hydrological and flood conditions in the Cambodian Mekong floodplain could
482 imply both positive and negative consequences to various sectors such as water resource
483 management, agricultural productions, and ecosystem services (Arias et al., 2012; Kummur and
484 Sarkkula, 2008). In addition, the direction, magnitude, and frequency of impacts will be varied
485 from one location to another.

486 The beneficial consequences associated with the impact of planned developments are
487 derived from increased water availability in the dry season, and reduced flood prevalence in
488 the wet season. The reduction in flood risk due to the decline in the wet season flows and water
489 levels would be a large socio-economic benefit of these development plans, potentially
490 reducing the duration and extent of affected regions by more than 20% (Fig. 5). In addition,
491 increased dry season flow would greatly enhance agricultural productivity, enhance water
492 security, and minimize conflicts between consumers. Environmental flow could also be secured
493 which may help some aspects of ecosystem productivity. Increases in water levels might also
494 reduce energy costs associated with water pumping, and better facilitate dry season navigation.

Formatted: Font color: Black

Formatted: Normal, Border: Top: (No border), Bottom:
(No border), Left: (No border), Right: (No border),
Between : (No border), Tab stops: 7.96 cm, Centered +
15.92 cm, Right

495 However, there are many negative consequences to the reduction in flood extent and
496 duration associated with the planned development scenarios. Hydropower projects in the
497 Mekong are projected to trap considerable parts of the sediments and the nutrients it contains
498 in the reservoir behind the dam wall, reducing their transportation downstream and subsequent
499 distribution across the floodplain (Kondolf et al., 2018; Kummu et al., 2010; Schmitt et al.,
500 2018; Schmitt et al., 2017). The reduction in sediment transport rates associated with reduced
501 wet season flows and sediment trapping upstream inevitably leads to sediment-starved water
502 flow downstream. This in turn leads to increased rates of channel incision and accelerating
503 riverbank erosion as river waters gain in-situ material for transportation up to carrying capacity
504 (Darby et al., 2013; Morris, 2014). The drop in soil fertility (nutrient bound to sediment)
505 throughout the downstream floodplains would result in a great challenge for ecosystem
506 productivity (Arias et al., 2014), rice production (Boretti, 2020) and the sustainability of
507 flooded forests (rich habitats for fish and other species) (Arias et al., 2014). Dams also act as
508 barriers disturbing fish migration between upstream and downstream sections essential for
509 feeding and breeding, resulting in fisheries losses (Ziv et al., 2012). In addition, the increasing
510 dry season water levels will disturb various river works - for instance, the low water level
511 condition is favourable to river channel maintenance (dredging) and constructions of water
512 infrastructure, usually started and very active during the dry season months.

513 Whilst higher economic damages from flood disasters are proportional to extended
514 flooded areas, intensifying flood depths, and prolonging flood durations, there are
515 counteracting positive impacts associated with floods, including the transport of nutrients and
516 increased fisheries productivity. Increasing flood extents widen the coverage of fertile
517 agricultural land (Lamberts, 2008), which implies a more extensive production of rice - the
518 most important agricultural activity in the Cambodian Mekong floodplain. In contrast, a
519 substantial reduction in flooded area would lead to a fall in flooded forest, a rich habitat for
520 fish and other species (Arias et al., 2014; Kummu and Sarkkula, 2008), leading to a decline in
521 fisheries and ecosystem productivity in general. These benefits from an extended flood extent
522 need to be balanced against the detrimental impacts of deep flood depths and long flood
523 durations, which can be catastrophic to crop yields across the floodplains. Therefore, suitable
524 flood conditions should be well determined for a better trade-off with the developmental
525 impacts.

Formatted: Font color: Black

Formatted: Normal, Border: Top: (No border), Bottom: (No border), Left: (No border), Right: (No border), Between : (No border), Tab stops: 7.96 cm, Centered + 15.92 cm, Right

526 4.3. Limitations and perspectives for future research

527 Several studies have been conducted to understand hydrologic processes within the Cambodian
528 Mekong floodplain, Tonle Sap Lake Basin, and Vietnamese Mekong Delta. Different
529 considerations have been taken into account for the analysis in previous research; they include
530 but are not limited to (1) water infrastructure development, (2) climate change, (3) sea level
531 rise, (4) land use and land cover change, (5) population growth, and (6) climatic related
532 phenomena. However, the present study is targeted to gain insight into how the combination of
533 upstream hydropower development, irrigation expansion, and climate change will affect the
534 Cambodian Mekong floodplain in terms of hydrological and flood patterns. Under climate
535 change scenarios, the future rainfall and temperature were assumed respectively to be wetter
536 and warmer.

537 Future research should employ finer resolution climate models and newer CMIP-6
538 scenarios, although according to our analysis of basin-wide mean precipitation and temperature
539 do not differ greatly between these two climate change modelling phases (Table S1). In
540 addition, a small-scale decision support tool set-up; as well as satellite-based image analysis to
541 assist in evaluating a comprehensive study of the flood vulnerability in the Cambodian Mekong
542 floodplain or the wider implications for the Water-Energy-Food Nexus for present and future
543 conditions.

544 Another relevant research direction is the prediction of future land use and river
545 morphological changes. This could generate a key input for a more realistic assessment of
546 hydrological and flood alterations. River sand mining has been very active in the Cambodian
547 Mekong River and its main tributaries as rapid and on-going urbanization requires a massive
548 amount of sand, which is an important material not only for construction but also for backfill
549 (Boretti, 2020; Hackney et al., 2020). Riverbank collapses, directly or indirectly associated
550 with excessive sand extraction, have been very severe. Moreover, many floodplains and
551 wetlands have been filled by sand and transformed into urban areas, resulting in a critical
552 change in river morphology and landscape along the river channels and throughout the
553 floodplains. More importantly, these alterations are still being perpetuated without the full
554 impact of their occurrence being understood or accounted for.

555 Floods are an essential component of the landscape for both the people and the
556 ecosystem of the Mekong Basin, but they also pose significant hazards and losses when the
557 magnitude is too great to handle effectively. As the development of water infrastructure could

Formatted: Font color: Black

Formatted: Normal, Border: Top: (No border), Bottom: (No border), Left: (No border), Right: (No border), Between : (No border), Tab stops: 7.96 cm, Centered + 15.92 cm, Right

558 cause a decrease in flood conditions and climate change may reverse such impacts, it is still
559 unknown what the desired flood water level and flood duration should be. This has led to a
560 great difficulty in proposing optimum flood protection measures while maximizing dam
561 benefits. Therefore, another potential research topic is the determination of the ideal flood
562 conditions for maximum productivity from both the agricultural and ecosystem perspectives.

563 The intended purpose of these future research is to provide valuable information and
564 assist governments, policymakers, and water resources engineers to foresee future threats of
565 different intensities. Moreover, their results would be helpful in formulating better water
566 resources management strategies, and in elevating all living things' resilience to the future
567 challenges for the sustainability of resources within the floodplain.

568 **5. Conclusions**

569 By combining the effects of development activities and climate change, this research
570 uses a novel setup of three different models to assess the potential impacts of hydropower
571 development, irrigation expansion, and climate change on the Cambodian Mekong floodplain.
572 We show through model validation that the developed modelling setup performs well in the
573 study area and could therefore potentially be used for future studies in the Mekong, as well as
574 in the floodplains of other large rivers. Our findings contribute to the delivery of more precise
575 information about the expected changes to flooding regimes in the area and highlight the
576 importance of properly characterising the directions and magnitudes of these changes. The
577 combined development scenarios that we analysed exhibited the same pattern of decreasing
578 hydrological conditions during the wet season, whilst increasing water discharge and water
579 levels in the dry season. The degree of hydrological alteration under hydropower development
580 and irrigation expansion is counteracted to a limited degree by the impact of future climate
581 change, which is projected to intensify the onset of wet season months and exacerbate water
582 deficiencies in the dry season months.

583 Our findings assist in strategic plan formulation and decision-making processes in the
584 dynamic Mekong region. The positive and negative implications of developmental impacts on
585 water availability, flow alterations, and particularly flood regime alterations should be carefully
586 considered when determining the level of investment to place in counteracting measures.
587 Reduced flooding during the wet season has flood protection benefits, whereas increases in dry
588 season flows have the benefit of increased water availability for irrigation. However, the

Formatted: Font color: Black

Formatted: Normal, Border: Top: (No border), Bottom:
(No border), Left: (No border), Right: (No border),
Between : (No border), Tab stops: 7.96 cm, Centered +
15.92 cm, Right

589 negative impacts should also be considered: a reduction in fisheries productivity, sediment
590 trapping and a decline in nutrient supply to the floodplain, and a reduction in floodplain
591 ecosystem productivity. Balancing these trade-offs will be an essential component of any
592 successful floodplain management strategy put in place to address future climate change and
593 uncertainty in a sustainable manner. A timely preparedness will be essential to avoid future
594 economic and environmental damages, as well as safeguarding the wellbeing of vulnerable
595 communities living throughout the Cambodian Mekong floodplain.

596

597 **Acknowledgements**

598 The study was funded by Academy of Finland funded project WASCO (grant no. 305471) and
599 additional funding was received from European Research Council (ERC) under the European
600 Union’s Horizon 2020 research and innovation programme (grant agreement No. 819202).
601 Authors are also sincerely thankful to all relevant organizations for supporting information and
602 data to conduct this study. The study has been greatly improved by the careful consideration
603 and comments made by two anonymous reviewers.

604

605 **References**

606 Adamson, P.T., Rutherford, I.D., Peel, M.C. & Conlan, I.A., 2009. Chapter 4 - The
607 Hydrology of the Mekong River, in: Campbell, I.C. (Eds.), The Mekong Academic
608 Press, San Diego, pp. 53-76.

609 ADB, 2004. Cumulative Impact Analysis and Nam Theun 2 Contributions - Final Report.
610 NORPLAN and EcoLao, Lao PDR.

611 Arias, M.E., Cochrane, T.A., Kumm, M., Lauri, H., Holtgrieve, G.W., Koponen, J. &
612 Piman, T., 2014. Impacts of hydropower and climate change on drivers of ecological
613 productivity of Southeast Asia's most important wetland. *Ecol. Modell.* 272, 252-263.
614 <https://doi.org/10.1016/j.ecolmodel.2013.10.015>.

615 Arias, M.E., Cochrane, T.A., Piman, T., Kumm, M., Caruso, B.S. & Killeen, T.J., 2012.
616 Quantifying changes in flooding and habitats in the Tonle Sap Lake (Cambodia)
617 caused by water infrastructure development and climate change in the Mekong Basin.
618 *Environ. Manage.* 112, 53-66. <https://doi.org/10.1016/j.jenvman.2012.07.003>.

619 ASABE, 2017. Guidelines for Calibrating, Validating, and Evaluating Hydrologic and Water
620 Quality (H/WQ) Models. 621, 1-15.

621 Benaman, J., Shoemaker, C.A. & Haith, D.A., 2005. Calibration and Validation of Soil and
622 Water Assessment Tool on an Agricultural Watershed in Upstate New York. *J.*
623 *Hydrol. Eng.* 10, 363-374. [https://doi.org/10.1061/\(ASCE\)1084-](https://doi.org/10.1061/(ASCE)1084-0699(2005)10:5(363))
624 [0699\(2005\)10:5\(363\)](https://doi.org/10.1061/(ASCE)1084-0699(2005)10:5(363)).

625 Boretti, A., 2020. Implications on food production of the changing water cycle in the
626 Vietnamese Mekong Delta. *Glob. Ecol. Conserv.* 22, e00989.
627 <https://doi.org/10.1016/j.gecco.2020.e00989>.

628 Chen, A., Liu, J., Kumm, M., Varis, O., Tang, Q., Mao, G., Wang, J., & Chen, D., 2021.
629 Multidecadal variability of the Tonle Sap Lake flood pulse regime. *Hydrological*
630 *Processes*, 35(9). <https://doi.org/10.1002/hyp.14327>

631 Dang, T.D., Cochrane, T.A., Arias, M.E. & Tri, V.P.D., 2018. Future hydrological alterations
632 in the Mekong Delta under the impact of water resources development, land
633 subsidence and sea level rise. *J. Hydrol. Reg. Stud.* 15, 119-133.
634 <https://doi.org/10.1016/j.ejrh.2017.12.002>.

635 Darby, S.E., Leyland, J., Kumm, M., Räsänen, T.A. & Lauri, H., 2013. Decoding the drivers
636 of bank erosion on the Mekong river: The roles of the Asian monsoon, tropical
637 storms, and snowmelt. *Water Resour. Res.* 49, 2146-2163.
638 <https://doi.org/10.1002/wrcr.20205>.

639 Donchyts, G., Schellekens, J., Winsemius, H., Eisemann, E. & Van de Giesen, N., 2016. A 30
640 m Resolution Surface Water Mask Including Estimation of Positional and Thematic
641 Differences Using Landsat 8, SRTM and OpenStreetMap: A Case Study in the
642 Murray-Darling Basin, Australia. *Remote Sens.* 8, 386.

643 Dung, N.V., Merz, B., Bárdossy, A., Thang, T.D. and Apel, H., 2011. Multi-objective
644 automatic calibration of hydrodynamic models utilizing inundation maps and gauge
645 data. *Hydrology and Earth System Sciences*, 15(4), pp.1339-1354.

646 FAO, 2003. WRB Map of World Soil Resources. Food and Agriculture Organization of
647 United Nations (FAO), Land and Water Development Division.

648 Fischer, G., Tubiello, F. N., van Velthuisen, H., & Wiberg, D. A. 2007. Climate change
649 impacts on irrigation water requirements: Effects of mitigation, 1990–2080.
650 *Technological Forecasting and Social Change*, 74(7), 1083–1107.
651 <https://doi.org/10.1016/j.techfore.2006.05.021>

Formatted: Font color: Black

Formatted: Normal, Border: Top: (No border), Bottom: (No border), Left: (No border), Right: (No border), Between : (No border), Tab stops: 7.96 cm, Centered + 15.92 cm, Right

652 Fujii, H., Garsdal, H., Ward, P., Ishii, M., Morishita, K. & Boivin, T., 2003. Hydrological
 653 roles of the Cambodian floodplain of the Mekong River. *Int. J. River Basin Manag.* 1,
 654 253-266. 10.1080/15715124.2003.9635211.
 655 GLC2000, 2003. Global Land Cover 2000 database. European Commission, Joint Research
 656 Centre.
 657 Hackney, C.R., Darby, S.E., Parsons, D.R., Leyland, J., Best, J.L., Aalto, R., Nicholas, A.P.
 658 & Houseago, R.C., 2020. River bank instability from unsustainable sand mining in the
 659 lower Mekong River. *Nat. Sustain.* 3, 217-225. 10.1038/s41893-019-0455-3.
 660 Her, Y., Yoo, S.-H., Cho, J., Hwang, S., Jeong, J. & Seong, C., 2019. Uncertainty in
 661 hydrological analysis of climate change: multi-parameter vs. multi-GCM ensemble
 662 predictions. *Sci. Rep.* 9, 4974. 10.1038/s41598-019-41334-7.
 663 Hoang, L.P., Lauri, H., Kumm, M., Koponen, J., van Vliet, M.T.H., Supit, I., Leemans, R.,
 664 Kabat, P. & Ludwig, F., 2016. Mekong River flow and hydrological extremes under
 665 climate change. *Hydrol. Earth Syst. Sci.* 20, 3027-3041. [https://doi.org/10.5194/hess-
 666 20-3027-2016](https://doi.org/10.5194/hess-20-3027-2016).
 667 Hoang, L.P., van Vliet, M.T.H., Kumm, M., Lauri, H., Koponen, J., Supit, I., Leemans, R.,
 668 Kabat, P. & Ludwig, F., 2019. The Mekong's future flows under multiple drivers:
 669 How climate change, hydropower developments and irrigation expansions drive
 670 hydrological changes. *Sci. Total Environ.* 649, 601-609.
 671 <https://doi.org/10.1016/j.scitotenv.2018.08.160>.
 672 Hoanh, C.T., Jirayoot, K., Lacombe, G. & Srinetr, V., 2010. Impacts of climate change and
 673 development on Mekong flow regimes. First assessment-2009. MRC Technical Paper
 674 No. 29, International Water Management Institute and Mekong River Commission,
 675 Vientiane, Lao PDR.
 676 ICEM & Alluvium, 2018. TA 9204-THA Strengthening Integrated Water Resource Planning
 677 and Management at River Basin Level. Asian Development Bank, Hanoi, Vietnam.
 678 [IPCC, 2014. Climate Change 2014: Synthesis Report. Contribution of Working Groups I, II
 679 and III to the Fifth Assessment Report of the Intergovernmental Panel on Climate
 680 Change. Geneva, Switzerland.](#)
 681 Jarvis, A., Reuter, H.I., Nelson, A. & Guevara, E., 2008. Hole-filled SRTM for the globe
 682 version 4: data grid. <http://srtm.csi.cgiar.org/> (accessed 2020).
 683 Ji, X., Li, Y., Luo, X. & He, D., 2018. Changes in the Lake Area of Tonle Sap: Possible
 684 Linkage to Runoff Alterations in the Lancang River? *Remote Sens.* 10, 866.
 685 Kallio, M., & Kumm, M., 2021. Comment on 'Changes of inundation area and water
 686 turbidity of Tonle Sap Lake: Responses to climate changes or upstream dam
 687 construction?' *Environmental Research Letters*, 16(5), 058001.
 688 <https://doi.org/10.1088/1748-9326/abf3da>
 689 Kazama, S., Hagiwara, T., Ranjan, P., & Sawamoto, M., 2007. Evaluation of groundwater
 690 resources in wide inundation areas of the Mekong River basin. *Journal of Hydrology*,
 691 340(3-4), 233-243. <https://doi.org/10.1016/j.jhydrol.2007.04.017>
 692 Kondolf, G.M., Schmitt, R.J.P., Carling, P., Darby, S., Arias, M., Bizzi, S., Castelletti, A.,
 693 Cochrane, T.A., Gibson, S., Kumm, M., Oeurng, C., Rubin, Z. & Wild, T., 2018.
 694 Changing sediment budget of the Mekong: Cumulative threats and management
 695 strategies for a large river basin. *Sci. Total Environ.* 625, 114-134.
 696 10.1016/j.scitotenv.2017.11.361.
 697 Kumm, M., Lu, X.X., Wang, J.J. & Varis, O., 2010. Basin-wide sediment trapping
 698 efficiency of emerging reservoirs along the Mekong. *Geomorphology (Amst)* 119,
 699 181-197. 10.1016/j.geomorph.2010.03.018.
 700 Kumm, M. & Sarkkula, J., 2008. Impact of the Mekong River Flow Alteration on the Tonle
 701 Sap Flood Pulse. *Ambio* 37, 185-192. <https://www.jstor.org/stable/25547881>.

Formatted: Swedish (Sweden)

Formatted: Font color: Black

Formatted: Normal, Border: Top: (No border), Bottom:
 (No border), Left: (No border), Right: (No border),
 Between : (No border), Tab stops: 7.96 cm, Centered +
 15.92 cm, Right

702 Lamberts, D., 2008. Little impact, much damage: the consequences of Mekong River flow
 703 alterations for the Tonle Sap ecosystem, in: Kumm, M., Keskinen, M., Varis, O.
 704 (Eds.), Modern Myths of the Mekong. A critical review of water and development
 705 concepts, principles and policies Water & Development Publications - Helsinki
 706 University of Technology, Helsinki, Finland, pp. 3-18.
 707 Lauri, H., Veijalainen, N., Kumm, M., Koponen, J., Virtanen, M., Inkala, A., Sark, J., 2006.
 708 VMod Hydrological Model Manual. Finnish Environment Institute, EIA Ltd.,
 709 Helsinki University of Technology.
 710 Lauri, H., Moel, H.d., Ward, P., Räsänen, T., Keskinen, M. & Kumm, M., 2012. Future
 711 changes in Mekong River hydrology: impact of climate change and reservoir
 712 operation on discharge. *Hydrol. Earth Syst. Sci.* 16, 4603-4619. 10.5194/hess-16-
 713 4603-2012.
 714 [Manh, N. V., Dung, N. V., Hung, N. N., Kumm, M., Merz, B., & Apel, H., 2015. Future
 715 sediment dynamics in the Mekong Delta floodplains: Impacts of hydropower
 716 development, climate change and sea level rise. *Global and Planetary Change*, 127,
 717 22–33. <https://doi.org/10.1016/j.gloplacha.2015.01.001>
 718 May, R., Jinno, K., & Tsutsumi, A., 2011. Influence of flooding on groundwater flow in
 719 central Cambodia. *Environmental Earth Sciences*, 63\(1\), 151–161.
 720 <https://doi.org/10.1007/s12665-010-0679-z>
 721 Morris, G.L., 2014. Sediment Management and Sustainable Use of Reservoirs, in: Wang,
 722 L.K., Yang, C.T. \(Eds.\), Modern Water Resources Engineering Humana Press,
 723 Totowa, New Jersey, pp. 279-337.
 724 MRC, 2009. Database of the Existing, Under Construction and Planned/Proposed
 725 Hydropower Projects in the Lower Mekong Basin. Mekong River Commission,
 726 Vientiane, Lao PDR.
 727 MRC, 2011. Annual Mekong Flood Report 2010. Mekong River Commission, Vientiane, Lao
 728 PDR.
 729 MRC, 2016. Mekong River Commission Contract No. 027-2015. Mekong River Commission,
 730 Vientiane, Lao PDR.
 731 MRC, 2017. THE COUNCIL STUDY: The Study on the Sustainable Management and
 732 Development of the Mekong River Basin including Impacts of Mainstream
 733 Hydropower Projects. Climate Change Report: Climate Change Impacts for Council
 734 Study Sectors, Mekong River Commission, Vientiane, Lao PDR.
 735 MRC, 2018a. THE COUNCIL STUDY: WUP-FIN IWRM Scenario Modelling Report.
 736 Mekong River Commission, Vientiane, Lao PDR.
 737 MRC, 2018b. MRC Council Study: Volume 1 Summary Modeling Report v2.0. Mekong
 738 River Commission, Vientiane, Lao PDR.
 739 MRC, 2019. Snapshot of the MRC Council Study* findings and recommendations. Mekong
 740 River Commission, Vientiane, Lao PDR.
 741 MRC, 2020. THE MRC HYDROPOWER MITIGATION GUIDELINES: Guidelines for
 742 Hydropower Environmental Impact Mitigation and Risk Management in the Lower
 743 Mekong Mainstream and Tributaries \(Vol. 3\), ed. Mekong River Commission,
 744 Vientiane, Lao PDR.
 745 Piman, T., Cochrane, T., Arias, M., Green, A. & Dat, N., 2013. Assessment of Flow Changes
 746 from Hydropower Development and Operations in Sekong, Sesan, and Srepok Rivers
 747 of the Mekong Basin. *J. Water Resour. Plan. Manag.* 139, 723-732.
 748 <https://doi.org/10.1061/ASCEWR.1943-5452.0000286>.
 749 Pokhrel, Y., Shin, S., Lin, Z., Yamazaki, D. & Qi, J., 2018. Potential Disruption of Flood
 750 Dynamics in the Lower Mekong River Basin Due to Upstream Flow Regulation. *Sci.*
 751 *Rep.* 8, 17767. 10.1038/s41598-018-35823-4.](#)

Formatted: Swedish (Sweden)

Formatted: Font color: Black

Formatted: Normal, Border: Top: (No border), Bottom:
 (No border), Left: (No border), Right: (No border),
 Between : (No border), Tab stops: 7.96 cm, Centered +
 15.92 cm, Right

752 Portmann, F. T., Siebert, S., & Döll, P., 2010. MIRCA2000-Global monthly irrigated and
 753 rainfed crop areas around the year 2000: A new high-resolution data set for
 754 agricultural and hydrological modeling. *Global Biogeochemical Cycles*, 24(1).
 755 <https://doi.org/10.1029/2008GB003435>
 756 Räsänen, T.A., Koponen, J., Lauri, H. & Kumm, M., 2012. Downstream Hydrological
 757 Impacts of Hydropower Development in the Upper Mekong Basin. *Water Resour.*
 758 *Manag.* 26, 3495-3513. <https://doi.org/10.1007/s11269-012-0087-0>.
 759 Rennó, C.D., Nobre, A.D., Cuatras, L.A., Soares, J.V., Hodnett, M.G., Tomasella, J. &
 760 Waterloo, M.J., 2008. HAND, a new terrain descriptor using SRTM-DEM: Mapping
 761 terra-firme rainforest environments in Amazonia. *Remote Sens. Environ.* 112, 3469-
 762 3481. <https://doi.org/10.1016/j.rse.2008.03.018>.
 763 Schmitt, R.J.P., Bizzi, S., Castelletti, A. & Kondolf, G.M., 2018. Improved trade-offs of
 764 hydropower and sand connectivity by strategic dam planning in the Mekong. *Nat.*
 765 *Sustain.* 1, 96-104. 10.1038/s41893-018-0022-3.
 766 Schmitt, R.J.P., Rubin, Z. & Kondolf, G.M., 2017. Losing ground - scenarios of land loss as
 767 consequence of shifting sediment budgets in the Mekong Delta. *Geomorphology*
 768 (Amst) 294, 58-69. <https://doi.org/10.1016/j.geomorph.2017.04.029>.
 769 Setegn, S.G., Dargahi, B., Srinivasan, R. & Melesse, A.M., 2010. Modeling of Sediment
 770 Yield From Anjeni-Gauged Watershed, Ethiopia Using SWAT Model. *J. Am. Water*
 771 *Resour. As.* 46, 514-526. <https://doi.org/10.1111/j.1752-1688.2010.00431.x>.
 772 Soukhaphon, A., Baird, I. G., & Hogan, Z. S., 2021. The Impacts of Hydropower Dams in the
 773 Mekong River Basin: A Review. *Water*, 13(3), 265.
 774 <https://doi.org/10.3390/w13030265>
 775 Tran, D.D., van Halsema, G., Hellegers, P.J.G.J., Phi Hoang, L., Quang Tran, T., Kumm, M.
 776 & Ludwig, F., 2018. Assessing impacts of dike construction on the flood dynamics
 777 of the Mekong Delta. *Hydrol. Earth Syst. Sci.* 22, 1875-1896. 10.5194/hess-22-1875-
 778 2018.
 779 Triet, N. V. K., Dung, N. V., Fujii, H., Kumm, M., Merz, B., & Apel, H., 2017. Has dyke
 780 development in the Vietnamese Mekong Delta shifted flood hazard downstream?
 781 *Hydrology and Earth System Sciences*, 21(8), 3991–4010.
 782 <https://doi.org/10.5194/hess-21-3991-2017>
 783 Triet, N.V.K., Dung, N.V., Hoang, L.P., Duy, N.L., Tran, D.D., Anh, T.T., Kumm, M.,
 784 Merz, B. & Apel, H., 2020. Future projections of flood dynamics in the Vietnamese
 785 Mekong Delta. *Sci. Total Environ.* 742, 140596.
 786 <https://doi.org/10.1016/j.scitotenv.2020.140596>.
 787 Try, S., Tanaka, S., Tanaka, K., Sayama, T., Lee, G. & Oeurng, C., 2020a. Assessing the
 788 effects of climate change on flood inundation in the lower Mekong Basin using high-
 789 resolution AGCM outputs. *Prog. Earth Planet. Sci.* 7, 34. 10.1186/s40645-020-00353-
 790 z.
 791 Try, S., Tanaka, S., Tanaka, K., Sayama, T., Oeurng, C., Uk, S., Takara, K., Hu, M. & Han,
 792 D., 2020b. Comparison of gridded precipitation datasets for rainfall-runoff and
 793 inundation modeling in the Mekong River Basin. *PLoS One* 15, e0226814-e0226814.
 794 10.1371/journal.pone.0226814.
 795 Västilä, K., Kumm, M., Sangmanee, C. & Chinvanno, S., 2010. Modelling climate change
 796 impacts on the flood pulse in the Lower Mekong floodplains. *J. Water Clim. Change*
 797 1, 67-86. <https://doi.org/10.2166/wcc.2010.008>.
 798 Xu, H., 2006. Modification of normalised difference water index (NDWI) to enhance open
 799 water features in remotely sensed imagery. *Int. J. Remote Sens.* 27, 3025-3033.
 800 <https://doi.org/10.1080/01431160600589179>.

Formatted: Swedish (Sweden)

Formatted: Finnish

Formatted: Swedish (Sweden)

Formatted: Font color: Black

Formatted: Normal, Border: Top: (No border), Bottom:
 (No border), Left: (No border), Right: (No border),
 Between : (No border), Tab stops: 7.96 cm, Centered +
 15.92 cm, Right

801 Yamazaki, D., Ikeshima, D., Tawatari, R., Yamaguchi, T., O'Loughlin, F., Neal, J.C.,
802 Sampson, C.C., Kanae, S. & Bates, P.D., 2017. A high-accuracy map of global terrain
803 elevations. Geophys. Res. Lett. 44, 5844-5853. <https://doi.org/10.1002/2017gl072874>.
804 Yu, W., Kim, Y., Lee, D. & Lee, G., 2019. Hydrological assessment of basin development
805 scenarios: Impacts on the Tonle Sap Lake in Cambodia. Quat. Int. 503, 115-127.
806 <https://doi.org/10.1016/j.quaint.2018.09.023>.
807 Ziv, G., Baran, E., Nam, S., Rodríguez-Iturbe, I. & Levin, S.A., 2012. Trading-off fish
808 biodiversity, food security, and hydropower in the Mekong River Basin. Proc. Natl.
809 Acad. Sci. U.S.A. 109, 5609-5614. 10.1073/pnas.1201423109.

810

811

|

Supplementary material

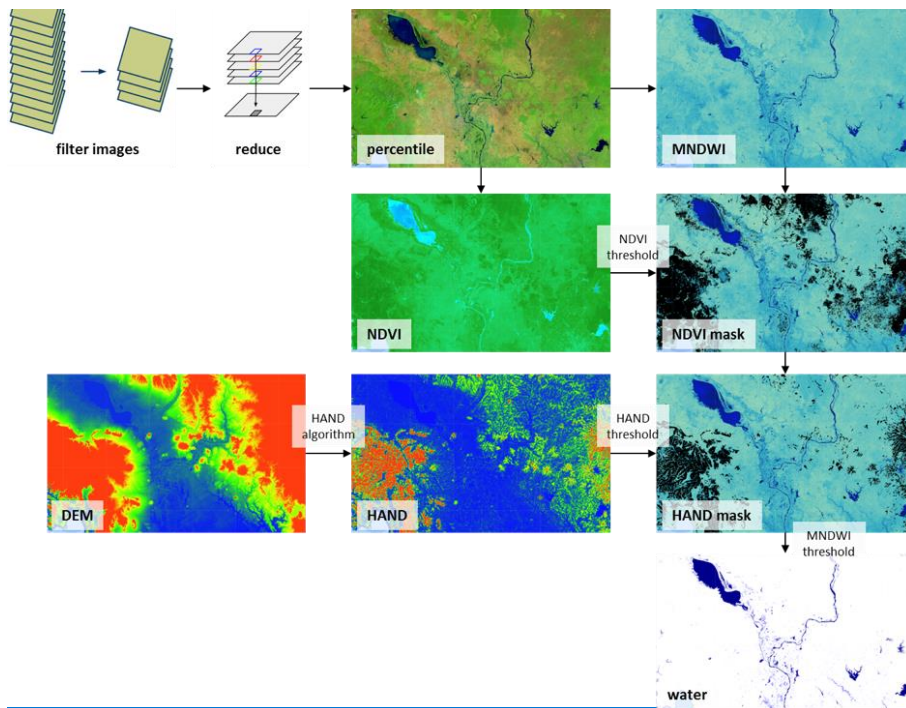
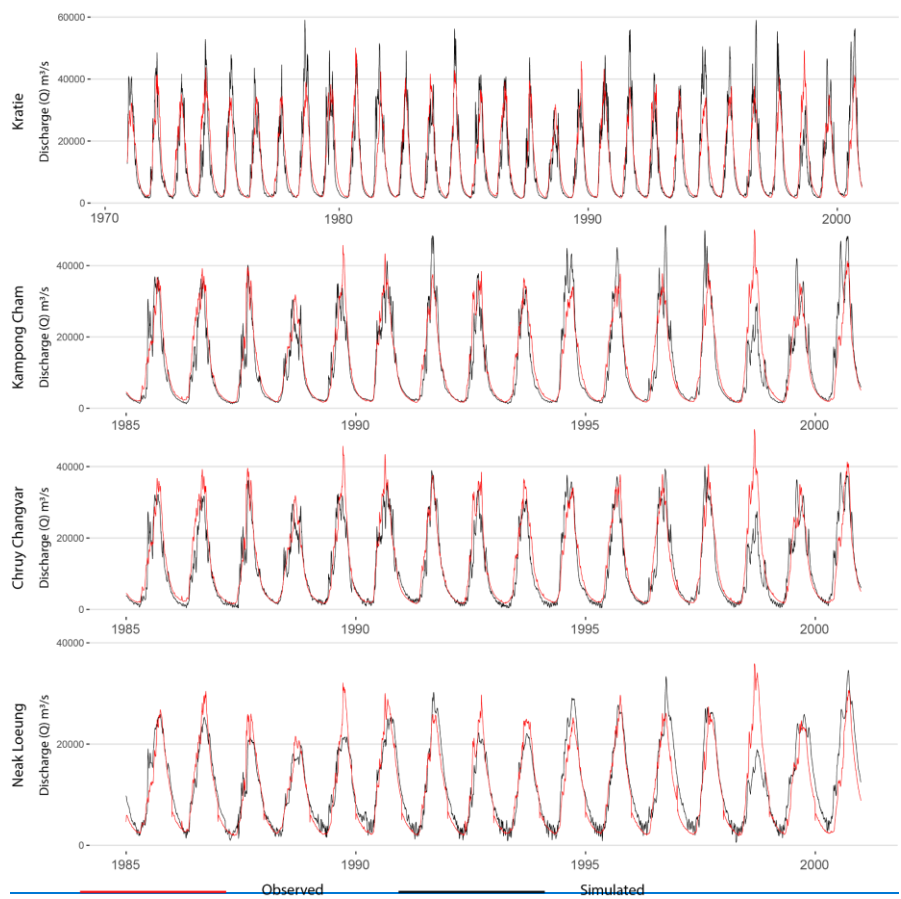


Fig. S1. Schematic processes in generating floodwater coverage from satellite images. MNDWI is the Modified Normalized Difference Water Index, NDVI is the Normalised Difference Vegetation Index, and HAND is the Height Above Nearest Drainage.

Formatted: Font color: Black

Formatted: Normal, Border: Top: (No border), Bottom: (No border), Left: (No border), Right: (No border), Between : (No border), Tab stops: 7.96 cm, Centered + 15.92 cm, Right

820



821

822 *Fig. S2. Time series comparison between the observed and simulated water discharge [Q] at each gauging station. See*
823 *location of the stations in Fig. 1.*

824

Formatted: Font color: Black

Formatted: Normal, Border: Top: (No border), Bottom: (No border), Left: (No border), Right: (No border), Between : (No border), Tab stops: 7.96 cm, Centered + 15.92 cm, Right

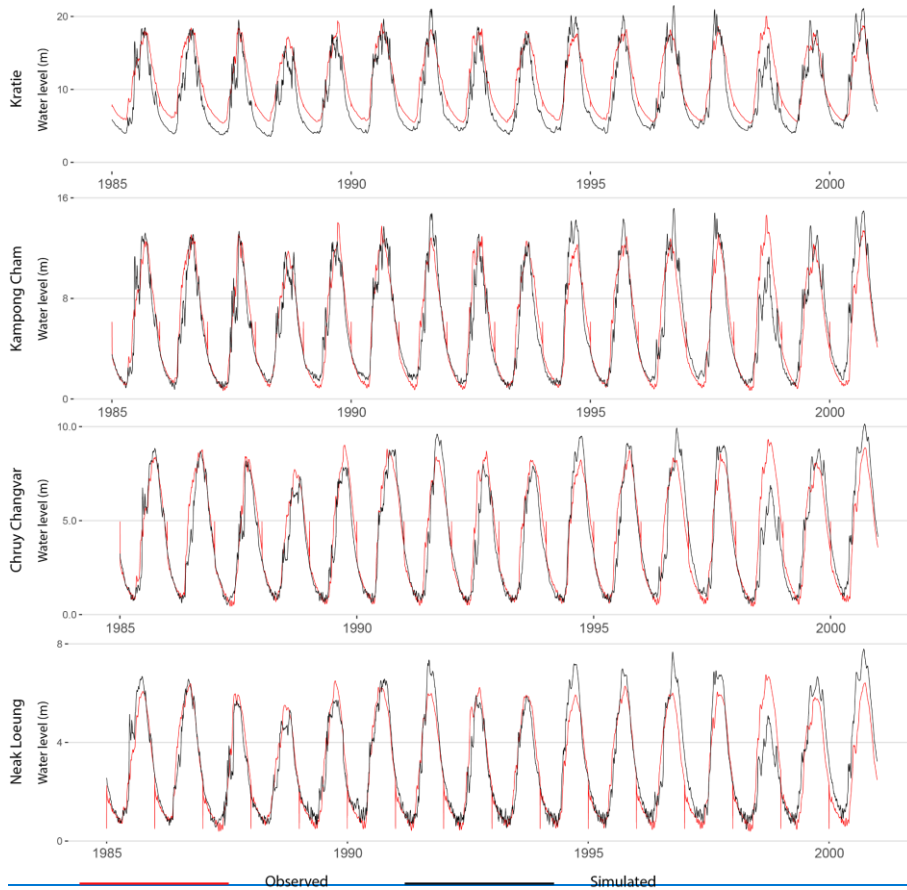


Fig. S3. Time series comparison between the observed and simulated water levels [WL] at each gauging station.

Formatted: Font color: Black

Formatted: Normal, Border: Top: (No border), Bottom: (No border), Left: (No border), Right: (No border), Between : (No border), Tab stops: 7.96 cm, Centered + 15.92 cm, Right

828 **Table S1.** Comparison of GCM ensemble means for precipitation and temperature across the
829 wet (May—Oct) and dry (Nov—Apr) seasons between CMIP 5 and CMIP 6. Analysis is
830 based on the ensemble median of six GCMs that are equivalent between CMIP5 and CMIP6
831 generations. Data with resolution of 5 arc min from www.worldclim.com were used.
832

	RCP 4.5		RCP 8.5	
	CMIP5	CMIP6	CMIP5	CMIP6
Precipitation—wet season (mm / 5 months)	1102	1086	1149	1090
Precipitation—dry season (mm / 7 months)	338	328	332	333
Temperature—wet season (°C)	23.6	23.6	24.0	24.1
Temperature—dry season (°C)	19.7	19.4	20.0	19.9

833
834

Formatted: Font color: Black

Formatted: Normal, Border: Top: (No border), Bottom: (No border), Left: (No border), Right: (No border), Between : (No border), Tab stops: 7.96 cm, Centered + 15.92 cm, Right